CHAPTER 4
CHARACTERISTICS OF PHOTOMULTIPLIER TUBES

This chapter details various characteristics of photomultiplier tubes, including basic and performance. For example, section 4.1 shows spectral response characteristics of typical photocathodes and also gives the definition of photocathode sensitivity and its measurement procedure. Section 4.2 explains dynode types, structures and typical characteristics. Section 4.3 describes various performance characteristics such as time response, operating stability, sensitivity, uniformity, and signal-to-noise ratio as well as their definitions, measurement procedures and specific product examples. It also provides precautions and suggestions for use.

4.1 Basic Characteristics of Photocathodes

This section introduces photocathodes and window materials which have been used in practical applications from the past to the present and also explains the terms used to define photocathodes such as quantum efficiency, radiant sensitivity, and luminous sensitivity.

4.1.1 Photocathode materials

Most photocathodes[1)-15)] are made of compound semiconductors which consist of alkali metals with a low work function. There are approximately ten kinds of photocathodes currently employed in practical applications. Each photocathode is available as a transmission (semitransparent) type or a reflection (opaque) type, with different device characteristics. In the early 1940's, the JEDEC (Joint Electron Devices Engineering Council) introduced the "S number" to designate photocathode spectral response which is classified by the combination of the photocathode and window material. Presently, since many photocathode and window materials are available, the "S number" is no longer frequently used except for S-1, S-20, etc. The photocathode spectral response is instead expressed in terms of material type. The photocathode materials commonly used in photomultiplier tubes are as follows.

(1) Cs-I

Cs-I is not sensitive to solar radiation and therefore often called "solar blind". Its sensitivity sharply falls off at wavelengths longer than 200 nanometers and it is exclusively used for vacuum ultraviolet detection. As a window material, MgF_2 crystals or synthetic silica are used because of high ultraviolet transmittance. Although Cs-I itself has high sensitivity to wavelengths shorter than 115 nanometers, the MgF_2 crystal used for the input window does not transmit wavelengths shorter than 115 nanometers.

To measure light with wavelengths shorter than 115 nanometers, an electron multiplier having a first dynode on which Cs-I is deposited is often used with the input window removed (in a vacuum).

(2) Cs-Te

Cs-Te is not sensitive to wavelengths longer than 300 nanometers and is also called "solar blind" just as with Cs-I. With Cs-Te, the transmission type and reflection type show the same spectral response range, but the reflection type exhibits higher sensitivity than the transmission type. Synthetic silica or MgF_2 is usually used for the input window.

(3) Sb-Cs

This photocathode has sensitivity in the ultraviolet to visible range, and is widely used in many applications. Because the resistance of the Sb-Cs photocathode is lower than that of the bialkali photocathode described later on, it is suited for applications where light intensity to be measured is relatively high so that a large current can flow in the cathode. Sb-Cs is also suitable for applications where the photocathode is cooled so its resistance becomes larger and causes problems with the dynamic range. Sb-Cs is chiefly used for reflection type photocathode.

(4) Bialkali (Sb-Rb-Cs, Sb-K-Cs)

Since two kinds of alkali metals are employed, these photocathodes are called "bialkali". The transmission type of these photocathodes has a spectral response range similar to the Sb-Cs photocathode, but has higher sensitivity and lower dark current. It also provides sensitivity that matches the emission of a NaI(Tl) scintillator, thus being widely used for scintillation counting in radiation measurements. On the other hand, the reflection-type bialkali photocathodes are fabricated by using the same materials, but different processing. As a result, they offer enhanced sensitivity on the long wavelength side, achieving a spectral response from the ultraviolet region to around 700 nanometers.

(5) High temperature, low noise bialkali (Sb-Na-K)

As with bialkali photocathodes, two kinds of alkali metals are used in this photocathode type. The spectral response range is almost identical to that of bialkali photocathodes, but the sensitivity is somewhat lower. This photocathode can withstand operating temperatures up to 175°C while other normal photocathodes are guaranteed to no higher than 50°C. For this reason, it is ideally suited for use in oil well logging where photomultiplier tubes are often subjected to high temperatures. In addition, when used at room temperatures, this photocathode exhibits very low dark current, which makes it very useful in low-level light measurement such as photon counting applications where low noise is a prerequisite.

(6) Multialkali (Sb-Na-K-Cs)

This photocathode uses three or more kinds of alkali metals. Due to high sensitivity over a wide spectral response range from the ultraviolet through near infrared region around 850 nanometers, this photocathode is widely used in broad-band spectrophotometers. Hamamatsu also provides a multialkali photocathode with long wavelength response extending out to 900 nanometers, which is especially useful in the detection of gas phase chemiluminescence in NOx, etc.

(7) Ag-O-Cs

Transmission type photocathodes using this material are sensitive from the visible through near infrared region, from 400 to 1200 nanometers, while the reflection type exhibits a slightly narrower spectral response region from 300 to 1100 nanometers. Compared to other photocathodes, this photocathode has lower sensitivity in the visible region, but it also provides sensitivity at longer wavelengths in the near infrared region. So both transmission and reflection type Ag-O-Cs photocathodes are chiefly used for near infrared detection.

(8) GaAsP (Cs)

A GaAsP crystal activated with cesium is used as a transmission type photocathode. This photocathode does not have sensitivity in the ultraviolet region but has a very high quantum efficiency in the visible region. Note that if exposed to incident light with high intensity, sensitivity degradation is more likely to occur when compared with other photocathodes composed of alkali metals.

(9) GaAs (Cs)

A GaAs crystal activated with cesium is used for both reflection type and transmission type photocathodes. The reflection type GaAs(Cs) photocathode has sensitivity across a wide range from the ultraviolet through near infrared region around 900 nanometers. It demonstrates a nearly flat, high-sensitivity spectral response curve from 300 and 850 nanometers. The transmission type has a narrower spectral response range because shorter wavelengths are absorbed. It should be noted that if exposed to incident light with high intensity, these photocathodes tend to suffer sensitivity degradation when compared with other photocathodes primarily composed of alkali metals.

(10) InGaAs (Cs)

This photocathode provides a spectral response extending further into the infrared region than the GaAs photocathode. Additionally, it offers a superior signal-to-noise ratio in the neighborhood of 900 to 1000 nanometers in comparison with the Ag-O-Cs photocathode.

(11) InP/InGaAsP(Cs), InP/InGaAs(Cs)

These are field-assisted photocathodes utilizing a PN junction formed by growing InP/InGaAsP or InP/InGaAs on an InP substrate. These photocathodes were developed by our own in-house semiconductor microprocess technology.[16) 17)] Applying a bias voltage to this photocathode lowers the conduction band barrier, and allows for higher sensitivity at long wavelengths extending to 1.4 μm or even 1.7 μm which have up till now been impossible to detect with a photomultiplier tube. Since these photocathodes produce large amounts of dark current when used at room temperatures, they must be cooled to between -60°C to -80°C during operation. The band model of these photocathodes is shown in Figure 4-1.

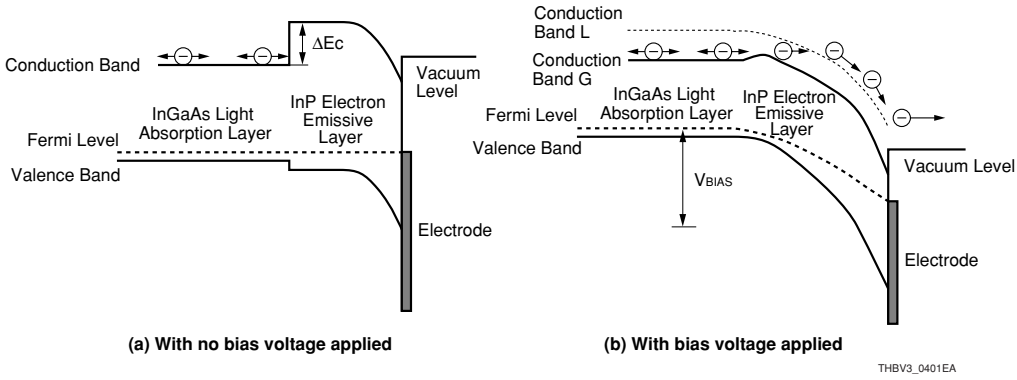

Figure 4-1: Band model

Typical spectral response characteristics of major photocathodes are illustrated in Figures 4-2 and 4-3 and Table 4-1. The JEDEC "S numbers" frequently used are also listed in Table 4-1. The definition of photocathode radiant sensitivity expressed in the ordinate of the figures is explained in section 4.1.3, "Spectral response characteristics". Note that Figures 4-2 and 4-3 and Table 4-1 only show typical characteristics and actual data may differ from tube to tube.

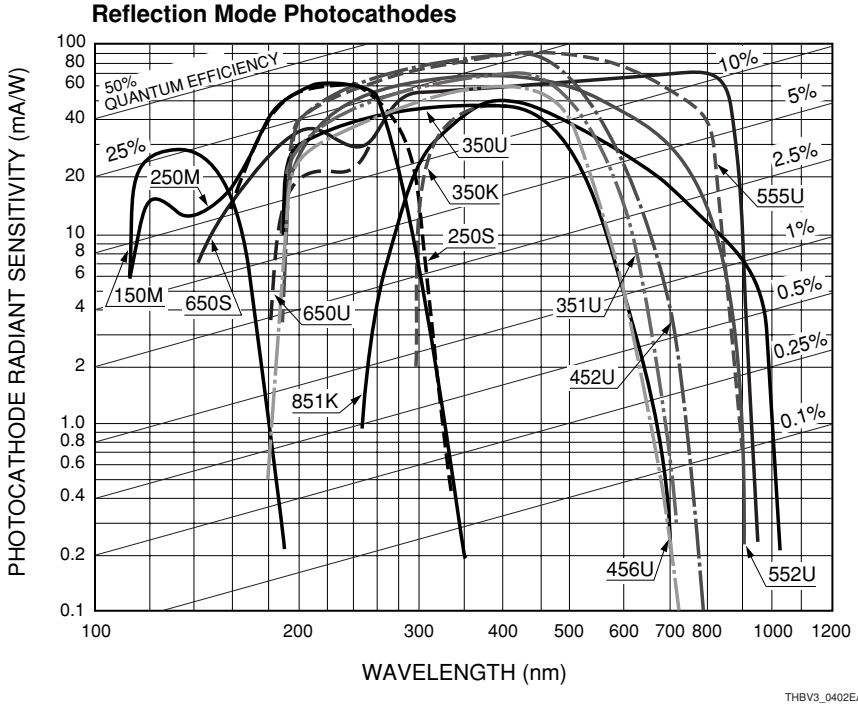

Figure 4-2 (a): Typical spectral response characteristics of reflection mode photocathodes

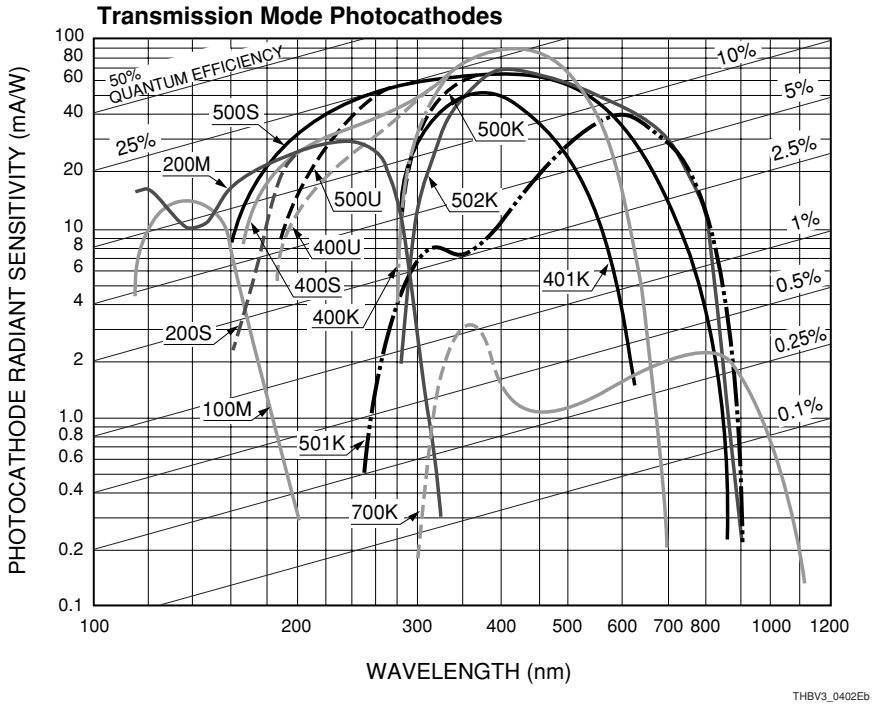

Figure 4-2 (b): Typical spectral response characteristics of transmission mode photocathodes

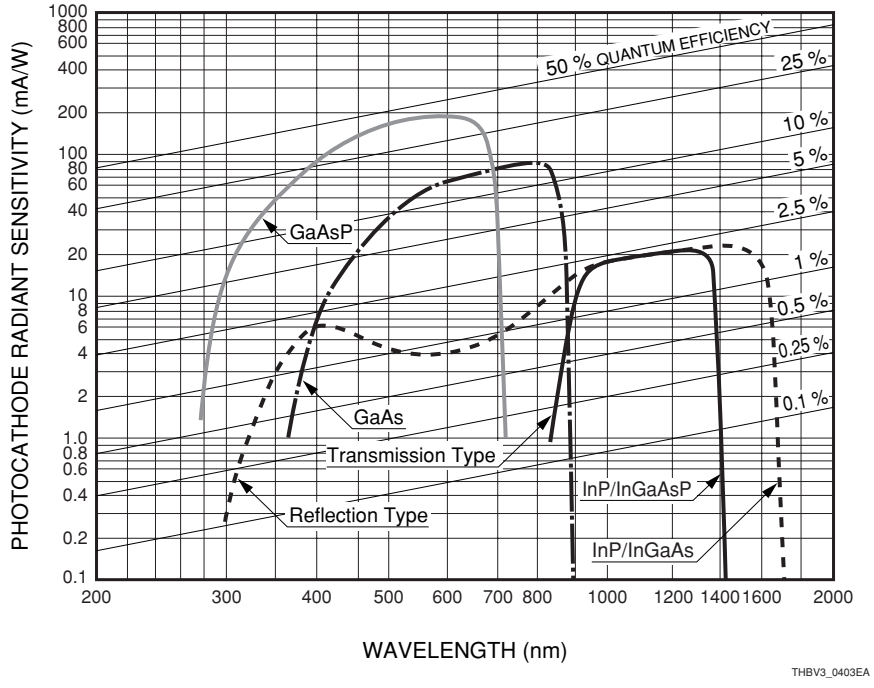

Figure 4-3: Typical spectral response characteristics of semiconductor crystal photocathodes

Reflection mode photocathodes

Curve Code (S number)	Photocathode Material	Window Material	Luminous Sensitivity (Typ.)	Spectral Response				
				Spectral Range	Peak Wavelength			
					Radiant Sensitivity		Quantum Efficiency	
			(μA/lm)	(nm)	(mA/W)	(nm)	(%)	(nm)
150M	Cs-I	MgF_2	—	115 to 200	25.5	135	26	125
250S	Cs-Te	Quartz	—	160 to 320	62	240	37	210
250M	Cs-Te	MgF_2	—	115 to 320	63	220	35	220
350K (S-4)	Sb-Cs	Borosilicate	40	300 to 650	48	400	15	350
350U (S-5)	Sb-Cs	UV	40	185 to 650	48	340	20	280
351U (Extd S-5)	Sb-Cs	UV	70	185 to 750	70	410	25	280
452U	Bialkali	UV	120	185 to 750	90	420	30	260
456U	Low dark bialkali	UV	60	185 to 680	60	400	19	300
552U	Multialkali	UV	200	185 to 900	68	400	26	260
555U	Multialkali	UV	525	185 to 900	90	450	30	260
650U	GaAs(Cs)	UV	550	185 to 930	62	300 to 800	23	300
650S	GaAs(Cs)	Quartz	550	160 to 930	62	300 to 800	23	300
851K	InGaAs(Cs)	Borosilicate	150	300 to 1040	50	400	16	370
—	InP/InGaAsP(Cs)	Borosilicate	—	300 to 1400	10	1250	1.0	1000 to 1200
—	InP/InGaAs(Cs)	Borosilicate	—	300 to 1700	10	1550	1.0	1000 to 1200

Table 4-1: Quick reference for typical spectral response characteristics (1)

Transmission mode photocathodes

Curve Code (S number)	Photocathode Material	Window Material	Luminous Sensitivity (Typ.)	Spectral Response				
				Spectral Range	Peak Wavelength			
					Radiant Sensitivity		Quantum Efficiency	
			(μA/lm)	(nm)	(mA/W)	(nm)	(%)	(nm)
100M	Cs-I	MgF_2	—	115 to 200	14	140	13	130
200S	Cs-Te	Quartz	—	160 to 320	29	240	14	210
200M	Cs-Te	MgF_2	—	115 to 320	29	240	14	200
400K	Bialkali	Borosilicate	95	300 to 650	88	420	27	390
400U	Bialkali	UV	95	185 to 650	88	420	27	390
400S	Bialkali	Quartz	95	160 to 650	88	420	27	390
401K	High temp. bialkali	Borosilicate	40	300 to 650	51	375	17	375
500K (S-20)	Multialkali	Borosilicate	150	300 to 850	64	420	20	375
500U	Multialkali	UV	150	185 to 850	64	420	25	280
500S	Multialkali	Quartz	150	160 to 850	64	420	25	280
501K (S-25)	Multialkali	Borosilicate	200	300 to 900	40	600	8	580
502K	Multialkali	Borosilicate (prism)	230	300 to 900	69	420	20	390
700K (S-1)	Ag-O-Cs	Borosilicate	20	400 to 1200	2.2	800	0.36	740
—	GaAsP(Cs)	—	—	300 to 720	180	580	40	540
—	GaAs(Cs)	—	—	380 to 890	85	800	14	760
—	InP/InGaAsP(Cs)	—	—	950 to 1400	21	1300	2.0	1000 to 1300
—	InP/InGaAs(Cs)	—	—	950 to 1700	24	1500	2.0	1000 to 1550

Table 4-1: Quick reference for typical spectral response characteristics (2)

4.1.2 Window materials

As stated in the previous section, most photocathodes have high sensitivity down to the ultraviolet region. However, because ultraviolet radiation tends to be absorbed by the window material, the short wavelength limit is determined by the ultraviolet transmittance of the window material.[18)-22)] The window materials commonly used in photomultiplier tubes are as follows:

(1) MgF_2 crystal

The crystals of alkali halide are superior in transmitting ultraviolet radiation, but have the disadvantage of deliquescence. A magnesium fluoride (MgF_2) crystal is used as a practical window material because it offers very low deliquescence and allows transmission of vacuum ultraviolet radiation down to 115 nanometers.

(2) Sapphire

Sapphire is made of Al_2O_3 crystal and shows an intermediate transmittance between the UV-transmitting glass and synthetic silica in the ultraviolet region. Sapphire glass has a short wavelength cutoff in the neighborhood of 150 nanometers, which is slightly shorter than that of synthetic silica.

(3) Synthetic silica

Synthetic silica transmits ultraviolet radiation down to 160 nanometers and in comparison to fused silica, offers lower levels of absorption in the ultraviolet region. Since silica has a thermal expansion coefficient greatly different from that of the Kovar alloy used for the stem pins (leads) of photomultiplier tubes, it is not suited for use as the bulb stem. As a result, a borosilicate glass is used for the bulb stem and then a graded seal, using glasses with gradually changing thermal expansion coefficient, is connected to the synthetic silica bulb, as shown in Figure 4-4. Because of this structure, the graded seal is very fragile and proper care should be taken when handling the tube. In addition, helium gas may permeate through the silica bulb and cause an increase in noise. Avoid operating or storing such tubes in environments where helium is present.

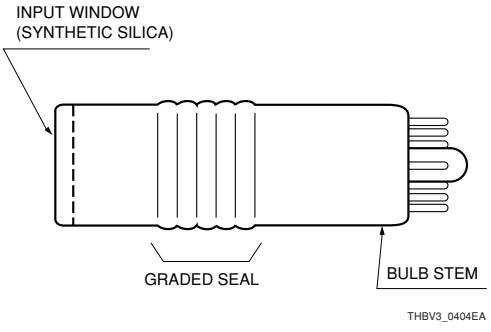

Figure 4-4: Grated seal

(4) UV glass (UV-transmitting glass)

As the name implies, this transmits ultraviolet radiation well. The short wavelength cutoff of the UV glass extends to 185 nanometers.

(5) Borosilicate glass

This is the most commonly used window material. Because the borosilicate glass has a thermal expansion coefficient very close to that of the Kovar alloy which is used for the leads of photomultiplier tubes, it is often called "Kovar glass". The borosilicate glass does not transmit ultraviolet radiation shorter than 300 nanometers. It is not suited for ultraviolet detection shorter than this wavelength. Moreover, some types of head-on photomultiplier tubes using a bialkali photocathode employ a special borosilicate glass (so-called "K-free glass") containing a very small amount of potassium (K^{40}) which may cause unwanted background counts. The K-free glass is mainly used for photomultiplier tubes designed for scintillation counting where

low background counts are desirable. For more details on background noise caused by K^{40}, refer to section 4.3.6, "Dark current".

Spectral transmittance characteristics of various window materials are shown in Figure 4-5.

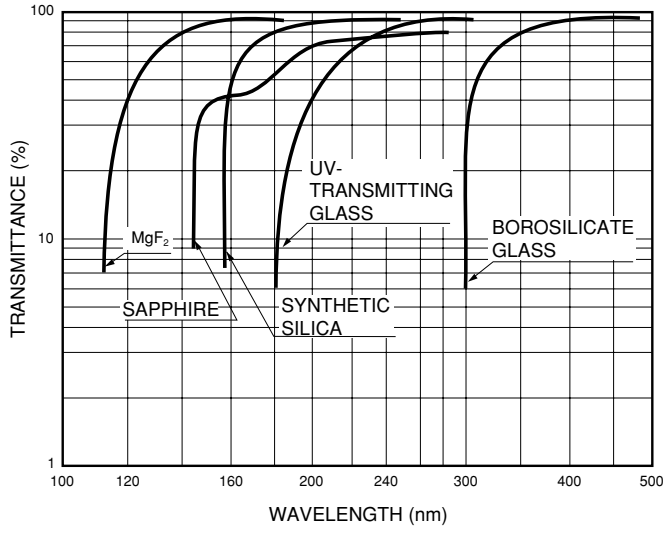

Figure 4-5: Spectral transmittance of window materials

4.1.3 Spectral response characteristics

The photocathode of a photomultiplier converts the energy of incident photons into photoelectrons. The conversion efficiency (photocathode sensitivity) varies with the incident light wavelength. This relationship between the photocathode and the incident light wavelength is referred to as the spectral response characteristics. In general, the spectral response characteristics are expressed in terms of radiant sensitivity and quantum efficiency.

(1) Radiant sensitivity

Radiant sensitivity is defined as the photoelectric current generated by the photocathode divided by the incident radiant flux at a given wavelength, expressed in units of amperes per watts (A/W). Furthermore, relative spectral response characteristics in which the maximum radiant sensitivity is normalized to 100% are also conveniently used.

(2) Quantum efficiency

Quantum efficiency is the number of photoelectrons emitted from the photocathode divided by the number of incident photons. Quantum efficiency is symbolized by η and is generally expressed as a percent. Incident photons transfer energy to electrons in the valence band of a photocathode, however not all of these electrons are emitted as photoelectrons. This photoemission takes place according to a certain probability process. Photons at shorter wavelengths carry higher energy compared to those at longer wavelengths and contribute to an increase in the photoemission probability. As a result, the maximum quantum efficiency occurs at a wavelength slightly shorter the wavelength of peak radiant sensitivity.

(3) Measurement and calculation of spectral response characteristics

To measure radiant sensitivity and quantum efficiency, a standard phototube or semiconductor detector which is precisely calibrated is used as a secondary standard. At first, the incident radiant flux L_p at the wavelength of interest is measured with the standard phototube or semiconductor detector. Next, the photomultiplier tube to be measured is set in place and the photocurrent Ik is measured. Then the radiant sensitivity Sk (A/W) of the photomultiplier tube can be calculated from the following equation:

$$Sk = \frac{I_K}{L_P} (A/W) \quad \text{(Eq. 4-1)}$$

The quantum efficiency η can be obtained from Sk using the following equation:

$$\eta(\%) = \frac{h \cdot c}{\lambda \cdot e} \cdot Sk = \frac{1240}{\lambda} \cdot Sk \cdot 100\% \quad \text{(Eq. 4-2)}$$

$h : 6.63 \times 10^{-34} J \cdot s$
$c : 3.00 \times 10^{8} m \cdot s^{-1}$
$e : 1.6 \times 10^{-19} C$

where h is Planck's constant, λ is the wavelength of incident light (nanometers), c is the velocity of light in vacuum and e is the electron charge. The quantum efficiency η is expressed in percent.

(4) Spectral response range (short and long wavelength limits)

The wavelength at which the spectral response drops on the short wavelength side is called the short wavelength limit or cutoff while the wavelength at which the spectral response drops on the long wavelength side is called the long wavelength limit or cutoff. The short wavelength limit is determined by the window material, while the long wavelength limit depends on the photocathode material. The range between the short wavelength limit and the long wavelength limit is called the spectral response range.

In this handbook, the short wavelength limit is defined as the wavelength at which the incident light is abruptly absorbed by the window material. The long wavelength limit is defined as the wavelength at which the photocathode sensitivity falls to 1 percent of the maximum sensitivity for bialkali and Ag-O-Cs photocathodes and 0.1 percent of the maximum sensitivity for multialkali photocathodes. However, these wavelength limits will depend on the actual operating conditions such as the amount of incident light, photocathode sensitivity, dark current and signal-to-noise ratio of the measurement system.

4.1.4 Luminous sensitivity

The spectral response measurement of a photomultiplier tube requires an expensive, sophisticated system and also takes much time. It is therefore more practical to evaluate the sensitivity of common photomultiplier tubes in terms of luminous sensitivity. The illuminance on a surface one meter away from a point light source of one candela (cd) is one lux. One lumen equals the luminous flux of one lux passing an area of one square meter. Luminous sensitivity is the output current obtained from the cathode or anode divided by the incident luminous flux (lumen) from a tungsten lamp at a distribution temperature of 2856K. In some cases, a visual-compensation filter is interposed between the photomultiplier tube and the light source, but in most cases it is omitted. Figure 4-6 shows the visual sensitivity and relative spectral distribution of a 2856K tungsten lamp.

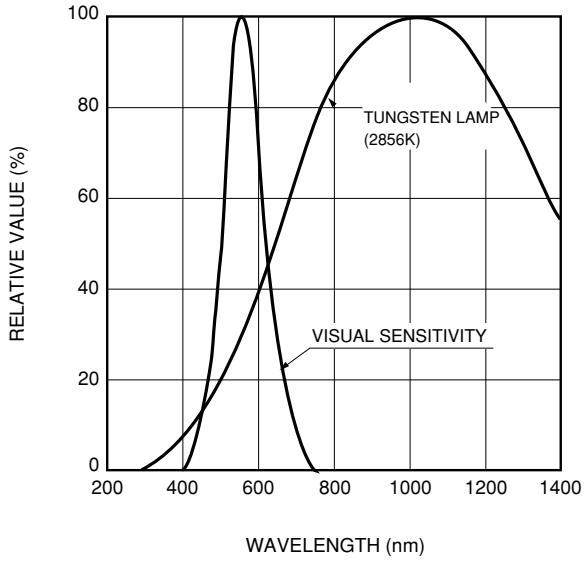

Figure 4-6: Response of eye and spectral distribution of 2856 K tungsten lamp

Luminous sensitivity is a convenient parameter when comparing the sensitivity of photomultiplier tubes of the same type. However, it should be noted that "lumen" is the unit of luminous flux with respect to the standard visual sensitivity and there is no physical significance for photomultiplier tubes which have a spectral response range beyond the visible region (350 to 750 nanometers). To evaluate photomultiplier tubes using Cs-Te or Cs-I photocathodes which are insensitive to the spectral distribution of a tungsten lamp, radiant sensitivity at a specific wavelength is measured.

Luminous sensitivity is divided into two parameters: cathode luminous sensitivity which defines the photocathode performance and anode luminous sensitivity which defines the performance characteristics after multiplication.

(1) Cathode luminous sensitivity

Cathode luminous sensitivity[23) 25)] is defined as the photoelectron current generated by the photocathode (cathode current) per luminous flux from a tungsten lamp operated at a distribution temperature of 2856K. In this measurement, each dynode is shorted to the same potential as shown in Figure 4-7, so that the photomultiplier tube is operated as a bipolar tube.

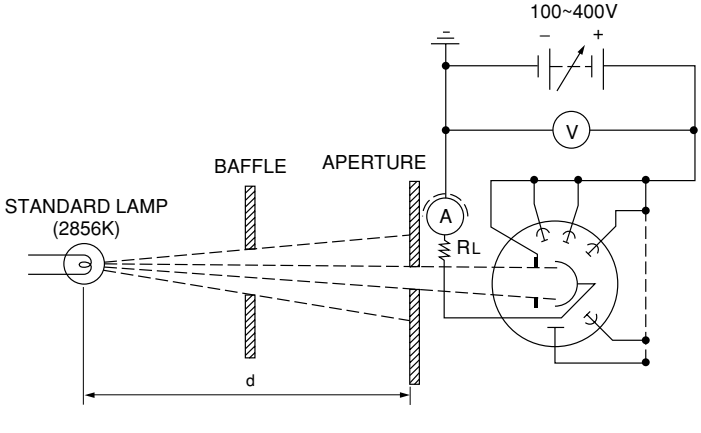

Figure 4-7: Cathode luminous sensitivity measuring diagram

The incident luminous flux used for measurement is in the range of 10^{-5} to 10^{-2} lumens. If the luminous flux is too large, measurement errors may occur due to the surface resistance of the photocathode. Consequently, the optimum luminous flux must be selected according to the photocathode size and material.

A picoammeter is usually used to measure the photocurrent which changes from several nanoamperes to several microamperes. Appropriate countermeasures against leakage current and other possible noise source must be taken. In addition, be careful to avoid contamination on the socket or bulb stem and to keep ambient humidity levels low so that an adequate electrical safeguard is provided.

The photomultiplier tube should be operated at a supply voltage at which the cathode current fully saturates. A voltage of 90 to 400 volts is usually applied for this purpose. Cathode saturation characteristics are discussed in section 4.3.2, "Linearity". The ammeter is connected to the cathode via a serial load resistance (R_L) of 100 kΩ to 1 MΩ for circuitry protection.

(2) Anode luminous sensitivity

Anode luminous sensitivity[23) 25)] is defined as the anode output current per luminous flux incident on the photocathode. In this measurement, a proper voltage distribution is given to each electrode as illustrated in Figure 4-8. Although the same tungsten lamp that was used to measure the cathode luminous sensitivity is used again, the light flux is reduced to 10^{-10} to 10^{-5} lumens using a neutral density filter. The ammeter is connected to the anode via the series resistance. The voltage-divider resistors used in this measurement must have minimum tolerance and good temperature characteristics.

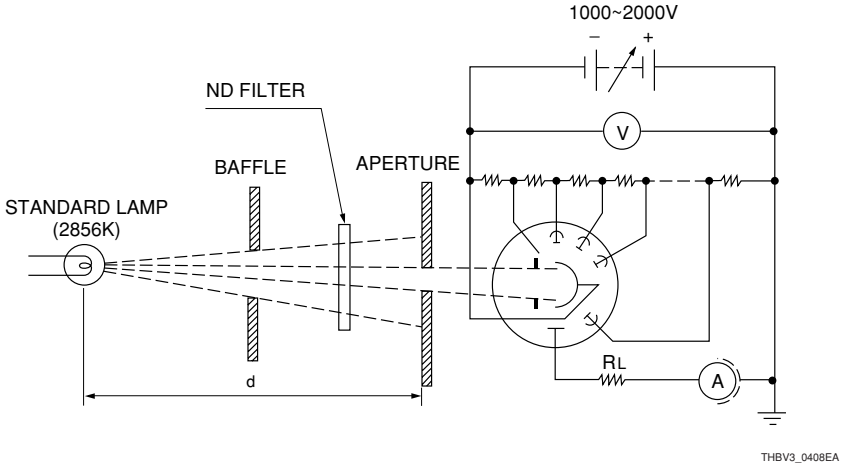

Figure 4-8: Anode luminous sensitivity measuring diagram

(3) Blue sensitivity index and red-to-white ratio

Blue sensitivity index and red-to-white ratio are often used for simple comparison of the spectral response of photomultiplier tubes.

Blue sensitivity is the cathode current obtained when a blue filter is placed in front of the photomultiplier tube under the same conditions for the luminous sensitivity measurement. The blue filter used is a Corning CS 5-58 polished to half stock thickness. Since the light flux entering the photomultiplier tube has been transmitted through the blue filter once, it cannot be directly represented in lumens. Therefore at Hamamatsu Photonics, it is expressed as a blue sensitivity index without using units. The spectral transmittance of this blue filter matches well the emission spectrum of a NaI(Tl) scintillator (peak wavelength 420 nanometers) which is widely used for scintillation counting. Photomultiplier tube sensitivity to the scintillation flash correlates well with the anode sensitivity using this blue filter. The blue sensitivity index is an important factor that affects energy resolution in scintillation measurement. For detailed information, refer to Chapter 7, "Scintillation counting".

The red-to-white ratio is used to evaluate photomultiplier tubes with a spectral response extending to the near infrared region. This parameter is defined as the quotient of the cathode sensitivity measured with a red or near infrared filter interposed under the same conditions for cathode luminous sensitivity divided by the cathode luminous sensitivity without a filter. The filter used is a Toshiba IR-D80A for Ag-O-Cs photocathodes or a Toshiba R-68 for other photocathodes. If other types of filters are used, the red-to-white ratio will vary. Figure 4-9 shows the spectral transmittance of these filters.

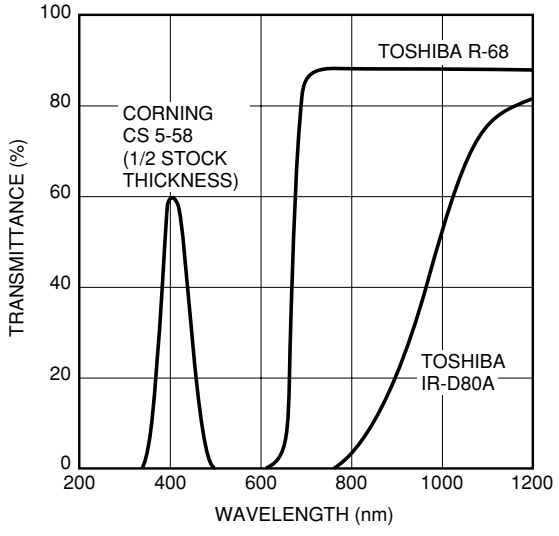

Figure 4-9: Typical spectral transmittance of optical filters.

4.1.5 Luminous sensitivity and spectral response

To some extent, there is a correlation between luminous sensitivity and spectral response at a specific wavelength. Figure 4-10 describes the correlation between luminous sensitivity, blue sensitivity index (CS 5-58) and red-to-white ratio (R-68, IR-D80A) as a function of wavelength.

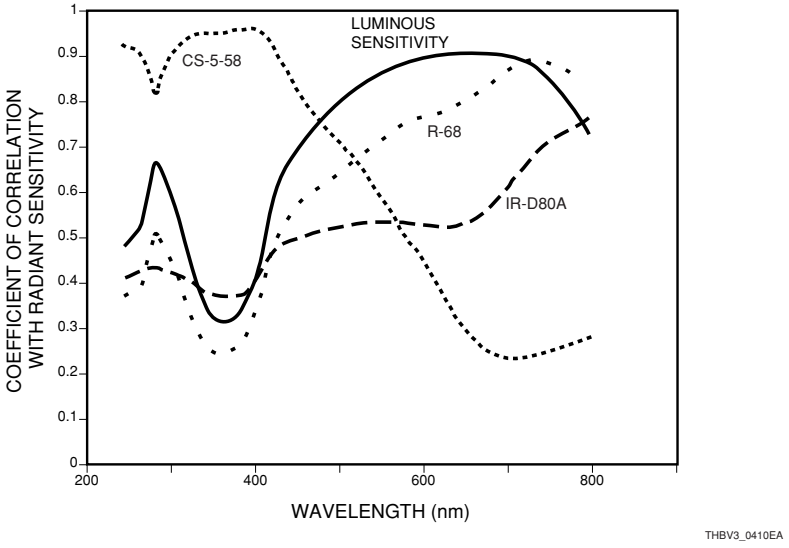

Figure 4-10: Correlation between luminous sensitivities and radiant sensitivity

It can be seen from the figure that the radiant sensitivity of a photomultiplier tube correlates well with the blue sensitivity index at wavelengths shorter than 450 nanometers, with the luminous sensitivity at 700 to 800 nanometers, with the red-to-white ratio using the Toshiba R-68 filter at 700 to 800 nanometers, and with the red-to-white ratio using the Toshiba IR-D80A filter at 800 nanometers or longer. From these correlation values, a photomultiplier tube with optimum sensitivity at a certain wavelength can be selected by simply measuring the sensitivity using a filter which has the best correlation value at that wavelength rather than measuring the spectral response.

4.2 Basic Characteristics of Dynodes

This section introduces typical dynode types currently in use and describes their basic characteristics: collection efficiency and gain (current amplification).

4.2.1 Dynode types and features

There are a variety of dynode types available and each type exhibits different gain, time response, uniformity and secondary-electron collection efficiency depending upon the structure and the number of stages. The optimum dynode type must be selected according to application. Figure 4-11 illustrates the cross sectional views of typical dynodes and their features are briefly discussed in the following sections. MCP-PMT's incorporating a microchannel plate for the dynode and photomultiplier tubes using a mesh dynode are respectively described in detail in Chapter 9 and Chapter 10. The electron bombardment type is explained in detail in Chapter 11.

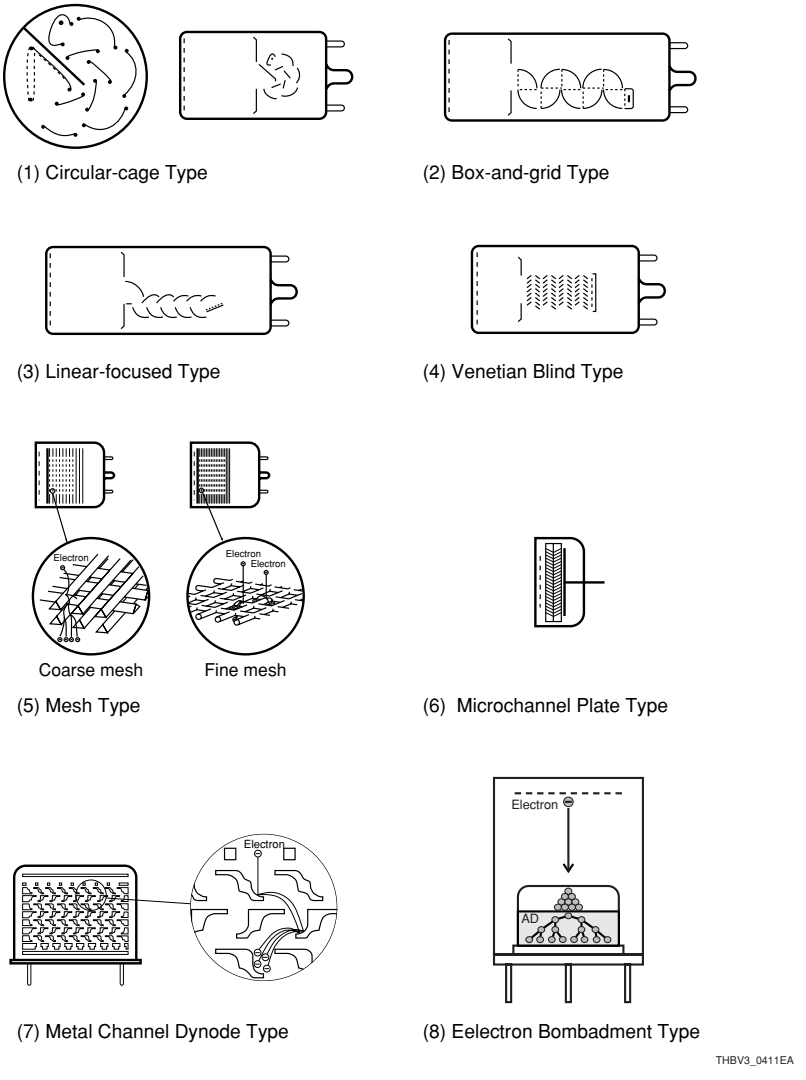

Figure 4-11: Types of electron multipliers

(1) Circular-cage type

The circular-cage type has an advantage of compactness and is used in all side-on photomultiplier tubes and in some head-on photomultiplier tubes. The circular-cage type also features fast time response.

(2) Box-and-grid type

This type, widely used in head-on photomultiplier tubes, is superior in photoelectron collection efficiency. Accordingly, photomultiplier tubes using this dynode offer high detection efficiency and good uniformity.

(3) Linear-focused type

As with the box-and-grid type, the linear-focused type is widely used in head-on photomultiplier tubes. Its prime features include fast time response, good time resolution and excellent pulse linearity.

(4) Venetian blind type

The venetian blind type creates an electric field that easily collects electrons, and is mainly used for head-on photomultiplier tubes with a large photocathode diameter.

(5) Mesh type

This type of dynode uses mesh electrodes stacked in close proximity to each other. There are two types: coarse mesh type and fine mesh type. Both are excellent in output linearity and have high immunity to magnetic fields. When used with a cross wire anode or multianode, the position of incident light can be detected. Fine mesh types are developed primarily for photomultiplier tubes which are used in high magnetic fields. (Refer to Chapter 9 for detailed information.)

(6) MCP (Microchannel plate)

A microchannel plate (MCP) with 1 millimeter thickness is used as the base for this dynode structure. This structure exhibits dramatically improved time resolution as compared to other discrete dynode structure. It also assures stable gain in high magnetic fields and provides position-sensitive capabilities when combined with a special anode. (Refer to Chapter 10 for detailed information.)

(7) Metal channel dynode

This dynode structure consists of extremely thin electrodes fabricated by our advanced micromachining technology and precisely stacked according to computer simulation of electron trajectories. Since each dynode is in close proximity to one another, the electron path length is very short ensuring excellent time characteristics and stable gain even in magnetic fields. (Refer to Chapter 9 for detailed information.)

(8) Electron bombardment type

In this type, photoelectrons are accelerated by a high voltage and strike a semiconductor so that the photoelectron energy is transferred to the semiconductor, producing a gain. This simple structure features a small noise figure, excellent uniformity and high linearity.

The electrical characteristics of a photomultiplier tube depend not only on the dynode type but also on the photocathode size and focusing system. As a general guide, Table 4-2 summarizes typical performance characteristics of head-on photomultiplier tubes (up to 2-inch diameter) classified by the dynode type. Magnetic characteristics listed are measured in a magnetic field in the direction of the most sensitive tube axis.

Dynode Type	Rise Time (ns)	Pulse Linearity at 2% (mA)	Magnetic Immunity (mT)	Uniform-ity	Collection Efficiency	Features
Circular-cage	0.9 to 3.0	1 to 10	0.1	Poor	Good	Compact, high speed
Box-and-grid	6 to 20			Good	Very good	High collection efficiency
Linear-focused	0.7 to 3	10 to 250		Poor	Good	High speed, high linearity
Venetian blind	6 to 18	10 to 40		Good	Poor	Suited for large diameter
Fine mesh	1.5 to 5.5	300 to 1000	500 to 1500*	Good	Poor	High magnetic immunity, high linearity
MCP	0.1 to 0.3	700	1500*	Good	Poor	high speed
Metal channel	0.65 to 1.5	30	5**	Good	Good	Compact, high speed
Electron bombardment type	Depends on internal semiconductor		—	Very good	Very good	High electron resolution

* In magnetic field parallel to tube axis
** Metal package PMT

Table 4-2: Typical characteristics for dynode types

4.2.2 Collection efficiency and gain (current amplification)

(1) Collection efficiency

The electron multiplier mechanism of a photomultiplier tube is designed with consideration to the electron trajectories so that electrons are efficiently multiplied at each dynode stage. However, some electrons may deviate from their favorable trajectories, not contributing to multiplication.

In general, the probability that photoelectrons will land on the effective area of the first dynode is termed the collection efficiency (α). This effective area is the area of the first dynode where photoelectrons can be multiplied effectively at the successive dynode stages without deviating from their favorable trajectories. Although there exist secondary electrons which do not contribute to multiplication at the second dynode or latter dynodes, they will tend to have less of an effect on the total collection efficiency as the number of secondary electrons emitted increases greatly. So the photoelectron collection efficiency at the first dynode is important. Figure 4-12 shows typical collection efficiency of a 28-mm diameter head-on photomultiplier tube (R6095) as a function of cathode-to-first dynode voltage. If the cathode-to-first dynode voltage is low, the number of photoelectrons that enter the effective area of the first dynode becomes low, resulting in a slight decrease in the collection efficiency.

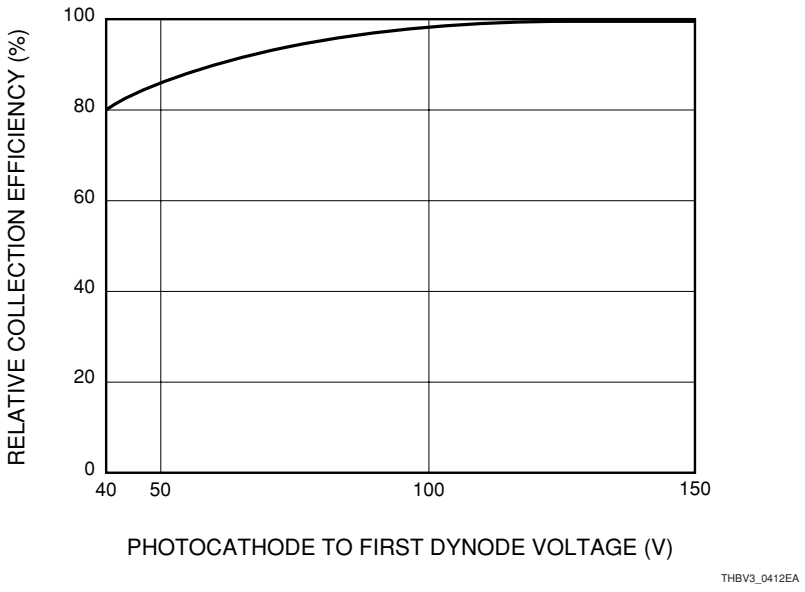

Figure 4-12: Collection efficiency vs. photocathode-to-first dynode voltage

Figure 4-12 shows that about 100 volts should be applied between the cathode and the first dynode. The collection efficiency influences energy resolution, detection efficiency and signal-to-noise ratio in scintillation counting. The detection efficiency is the ratio of the detected signal to the input signal of a photomultiplier tube. In photon counting this is expressed as the product of the photocathode quantum efficiency and the collection efficiency.

(2) Gain (current amplification)

Secondary emission ratio δ is a function of the interstage voltage of dynodes E, and is given by the following equation:

$$\delta = a \cdot E^{k} \quad \text{(Eq. 4-3)}$$

Where a is a constant and k is determined by the structure and material of the dynode and has a value from 0.7 to 0.8.

The photoelectron current Ik emitted from the photocathode strikes the first dynode where secondary electrons Idl are released. At this point, the secondary emission ratio δ_1 at the first dynode is given by

$$\delta_1 = \frac{I_{d1}}{I_K} \quad \text{(Eq. 4-4)}$$

These electrons are multiplied in a cascade process from the first dynode → second dynode → .... the n-th dynode. The secondary emission ratio δn of n-th stage is given by

$$\delta_n = \frac{I_{dn}}{I_{d(n-1)}} \quad \text{(Eq. 4-5)}$$

The anode current Ip is given by the following equation:

$$Ip = Ik \cdot \alpha \cdot \delta_1 \cdot \delta_2 \cdots \delta_n \quad \text{(Eq. 4-6)}$$

Then

$$\frac{Ip}{Ik} = \alpha \cdot \delta_1 \cdot \delta_2 \cdots \delta_n \quad \text{(Eq. 4-7)}$$

where α is the collection efficiency.

The product of α, δ_1, δ_2 .....δ n is called the gain μ (current amplification), and is given by the following equation:

$$\mu = \alpha \cdot \delta_1 \cdot \delta_2 \cdots \delta_n \quad \cdots\cdots \text{(Eq. 4-8)}$$

Accordingly, in the case of a photomultiplier tube with a=1 and the number of dynode stages = n, which is operated using an equally-distributed divider, the gain m changes in relation to the supply voltage V, as follows:

$$\mu = (a \cdot E^k)^n = a^n \left(\frac{V}{n+1}\right)^{kn} = A \cdot V^{kn} \quad \cdots\cdots \text{(Eq. 4-9)}$$

where A should be equal to $a^n/(n+1)^{kn}$. From this equation, it is clear that the gain μ is proportional to the kn exponential power of the supply voltage. Figure 4-13 shows typical gain vs. supply voltage. Since Figure 4-13 is expressed in logarithmic scale for both the abscissa and ordinate, the slope of the straight line becomes kn and the current multiplication increases with the increasing supply voltage. This means that the gain of a photomultiplier tube is susceptible to variations in the high-voltage power supply, such as drift, ripple, temperature stability, input regulation, and load regulation.

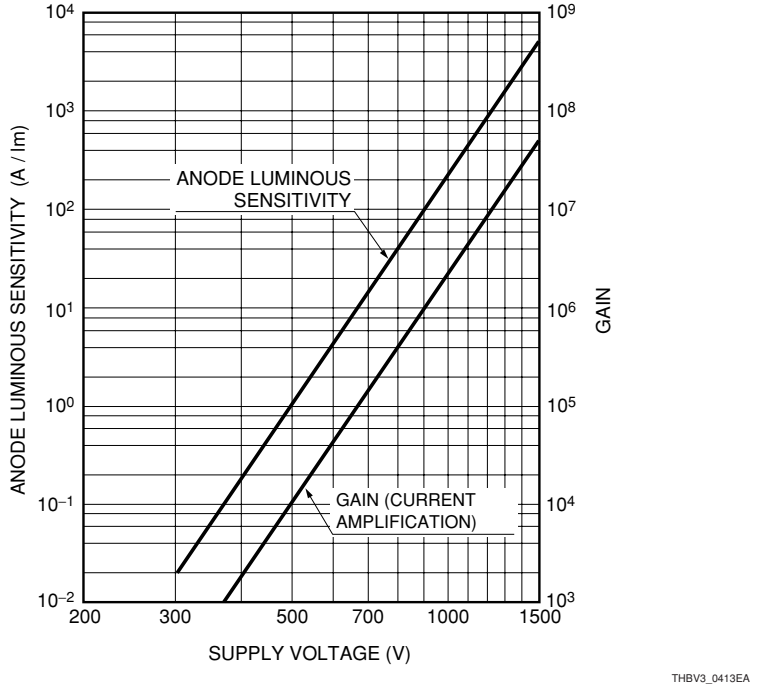

Figure 4-13: Gain vs. supply voltage

4.3 Characteristics of Photomultiplier Tubes

This section describes important characteristics for photomultiplier tube operation and their evaluation methods, and photomultiplier tube usage.

4.3.1 Time characteristics

The photomultiplier tube is a photodetector that has an exceptionally fast time response.[1) 23)-27)] The time response is determined primarily by the transit time required for the photoelectrons emitted from the photocathode to reach the anode after being multiplied as well as the transit time difference between each photoelectron. Accordingly, fast response photomultiplier tubes are designed to have a spherical inner window and carefully engineered electrodes so that the transit time difference can be minimized.

Table 4-3 lists the timing characteristics of 2-inch diameter head-on photomultiplier tubes categorized by their dynode type. As can be seen from the table, the linear-focused type and metal channel type exhibit the best time characteristics, while the box-and-grid and venetian blind types display rather poor properties.

Unit : ns

Dynode Type	Rise Time	Fall Time	Pulse Width (FWHM)	Electron Transit Time	TTS
Linear-focused	0.7 to 3	1 to 10	1.3 to 5	16 to 50	0.37 to 1.1
Circular-cage	3.4	10	7	31	3.6
Box-and-grid	to 7	25	13 to 20	57 to 70	Less than 10
Venetian blind	to 7	25	25	60	Less than 10
Fine mesh	2.5 to 2.7	4 to 6	5	15	Less than 0.45
Metal channel	0.65 to 1.5	1 to 3	1.5 to 3	4.7 to 8.8	0.4

Table 4-3: Typical time characteristics (2-inch dia. photomultiplier tubes)

The time response is mainly determined by the dynode type, but also depends on the supply voltage. Increasing the electric field intensity or supply voltage improves the electron transit speed and thus shortens the transit time. In general, the time response improves in inverse proportion to the square root of the supply voltage. Figure 4-14 shows typical time characteristics vs. supply voltage.

The following section explains and defines photomultiplier tube time characteristics and their measurement methods.

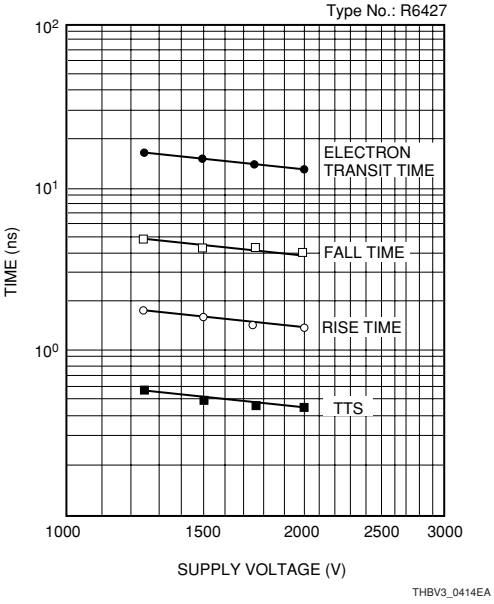

Figure 4-14: Time characteristics vs. supply voltage

(1) Rise time, fall time and electron transit time

Figure 4-15 shows a schematic diagram for time response measurements and Figure 4-16 illustrates the definitions of the rise time, fall time and electron transit time of a photomultiplier tube output.

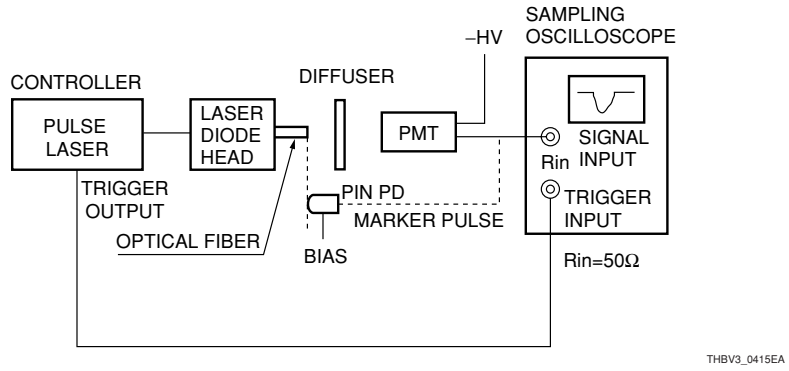

Figure 4-15: Measurement block diagram for rise/fall times and electron transit time

A pulsed laser diode is used as the light source. Its pulse width is sufficiently short compared to the light pulse width that can be detected by a photomultiplier tube. Thus it can be regarded as a delta-function light source. A sampling oscilloscope is used to sample the photomultiplier tube output many times so that a complete output waveform is created. The output signal generated by the photomultiplier tube is composed of waveforms which are produced by electrons emitted from every position of the photocathode. Therefore, the rise and fall times are mainly determined by the electron transit time difference and also by the electric field distribution and intensity (supply voltage) between the electrodes.

As indicated in Figure 4-16, the rise time is defined as the time for the output pulse to increase from 10 to 90 percent of the peak pulse height. Conversely, the fall time is defined as the time required to decrease from 90 to 10 percent of the peak output pulse height. In time response measurements where the rise and fall times are critical, the output pulse tends to suffer waveform distortion, causing an erroneous signal. To prevent this problem, proper impedance matching must be provided including the use of a voltage-divider circuit with damping resistors. (See Chapter 5.)

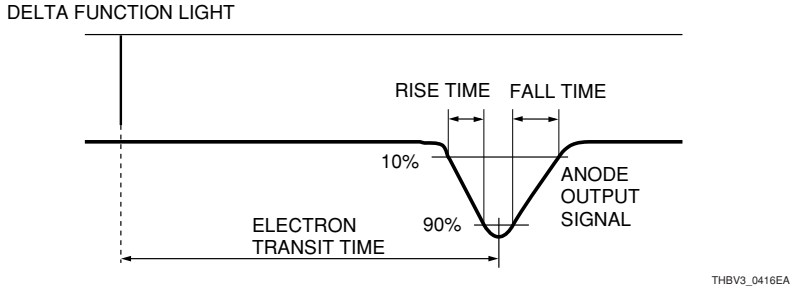

Figure 4-16: Definitions of rise/fall times and electron transit time

Figure 4-17 shows an actual output waveform obtained from a photomultiplier tube. In general, the fall time is two or three times longer than the rise time. This means that when measuring repetitive pulses, care must be taken so that each output pulse does not overlap. The FWHM (full width at half maximum) of the output pulse will usually be about 2.5 times the rise time.

The transit time is the time interval between the arrival of a light pulse at the photocathode and the appearance of the output pulse. To measure the transit time, a PIN photodiode is placed as reference (zero second) at the same position as the photomultiplier tube photocathode. The time interval between the instant the PIN photodiode detects a light pulse and the instant the output pulse of the photomultiplier tube reaches its peak amplitude is measured. This transit time is a useful parameter in determining the delay time of a measurement system in such applications as fluorescence lifetime measurement using repetitive light pulses.

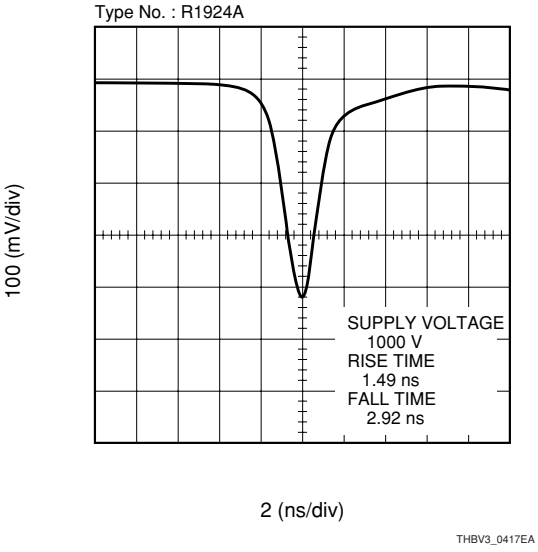

Figure 4-17: Output waveform

(2) TTS (transit time spread)

When a photocathode is fully illuminated with single photons, the transit time of each photoelectron pulse has a fluctuation. This fluctuation is called TTS (transit time spread). A block diagram for TTS measurement is shown in Figure 4-18 and typical measured data is shown in Figure 4-19.

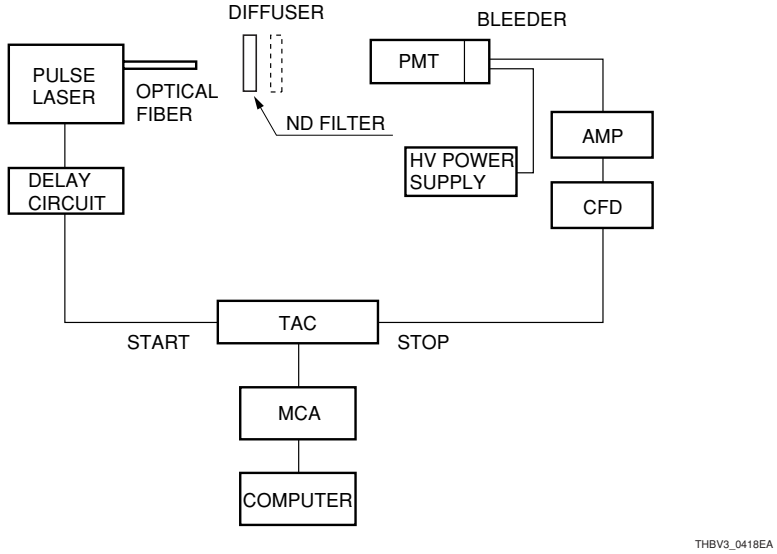

Figure 4-18: Block diagram for TTS measurement

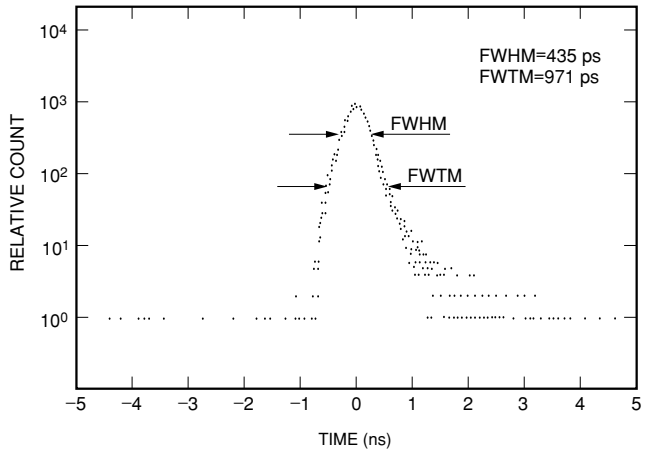

Figure 4-19: TTS (transit time spread)

In this measurement, a trigger signal from the pulsed laser is passed through the delay circuit and then fed as the start to the TAC (time-to-amplitude converter) which converts the time difference into pulse height. Meanwhile, the output from the photomultiplier tube is fed as the stop signal to the TAC via the CFD (constant fraction discriminator) which reduces the time jitter resulting from fluctuation of the pulse height. The TAC generates a pulse height proportional to the time interval between the "start" and "stop" signals. This pulse is fed to the MCA (multichannel analyzer) for pulse height analysis. Since the time interval between the "start" and "stop" signals corresponds to the electron transit time, a histogram displayed on the MCA, by integrating individual pulse height values many times in the memory, indicates the statistical spread of the electron transit time.

At Hamamatsu Photonics, the TTS is usually expressed in the FWHM of this histogram, but it may also be expressed in standard deviation. When the histogram shows a Gaussian distribution, the FWHM is equal to a value which is 2.35 times the standard deviation. The TTS improves as the number of photoelectrons per pulse increases, in inverse proportion to the square root of the number of photoelectrons. This relation is shown in Figure 4-20.

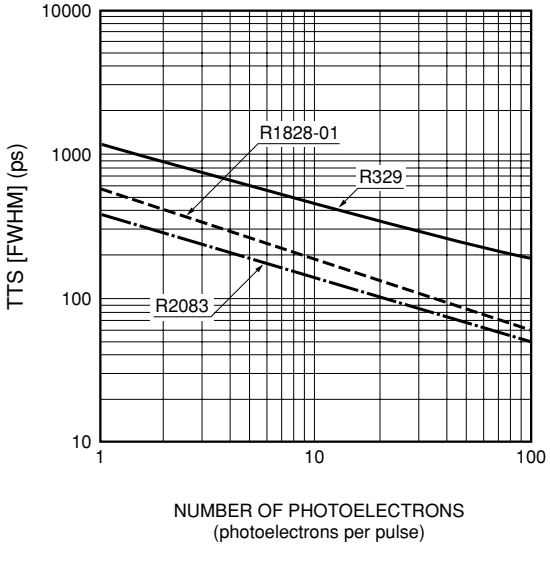

Figure 4-20: TTS vs. number of photoelectrons

(3) CTTD (cathode transit time difference)

The CTTD (cathode transit time difference) is the difference in transit time when the incident light position on the photocathode is shifted. In most time response measurements the entire photocathode is illuminated. However, as illustrated in Figure 4-21, the CTTD measurement employs an aperture plate to shift the position of a light spot entering the photocathode, and the transit time difference between each incident position is measured.

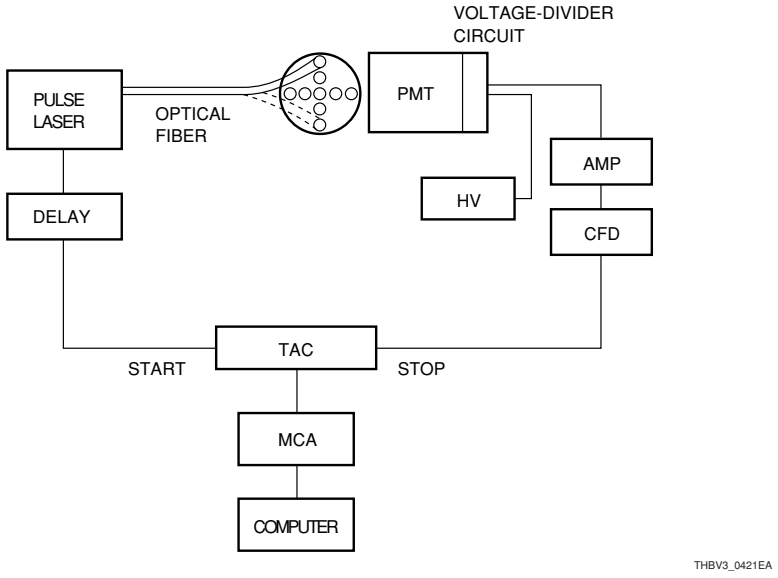

Figure 4-21: Block diagram for CTTD measurement

Basically, the same measurement system as for TTS measurement is employed, and the TTS histogram for each of the different incident light positions is obtained. Then the change in the peak pulse height of each histogram, which corresponds to the CTTD, is measured. The CTTD data of each position is represented as the transit time difference with respect to the transit time measured when the light spot enters the center of the photocathode.

In actual applications, the CTTD data is not usually needed but rather primarily used for evaluation in the photomultiplier tube manufacturing process. However, the CTTD is an important factor that affects the rise time, fall time and TTS described previously and also CRT (coincident resolving time) discussed in the next section.

(4) CRT (coincident resolving time)

As with the TTS, this is a measure of fluctuations in the transit time. The CRT measurement system resembles that used for positron CT or TOF (time of flight) measurement. Therefore, the CRT is a very practical parameter for evaluating the performance of photomultiplier tubes used in the above fields or similar applications. Figure 4-22 shows a block diagram of the CRT measurement.

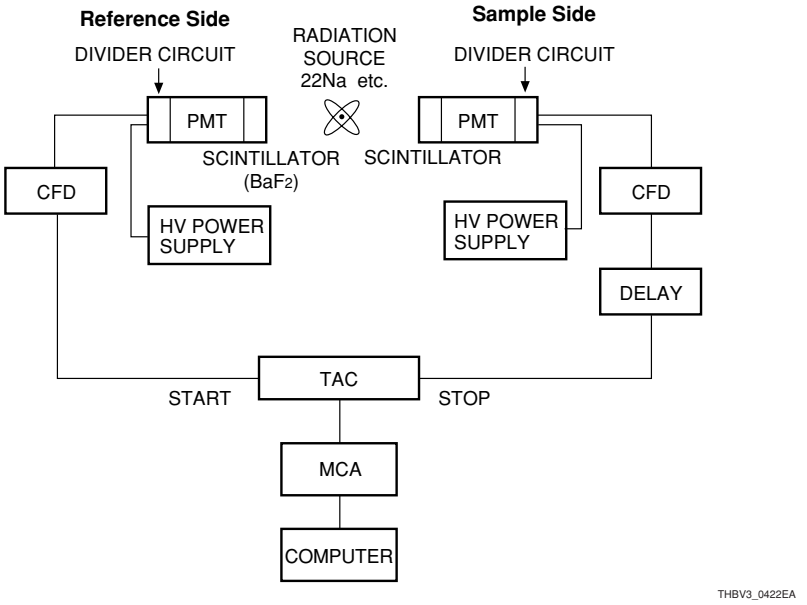

Figure 4-22: Block diagram for CRT measurement

As a radiation source ^{22}Na or ^{68}Ge-Ga is commonly used. As a scintillator, a BaF_2 is used on the reference side, while a BGO, BaF_2, CsF or plastic scintillator is used on the sample side. A proper combination of radiation source and scintillator should be selected according to the application. The radiation source is placed in the middle of a pair of photomultiplier tubes and emits gamma-rays in opposing directions at the same time. A coincident flash occurs from each of the two scintillators coupled to the photomultiplier tube. The signal detected by one photomultiplier tube is fed as the start signal to the TAC, while the signal from the other photomultiplier tube is fed as the stop signal to the TAC via the delay circuit used to obtain proper trigger timing. Then, as in the case of the TTS measurement, this event is repeatedly measured many times and the pulse height (time distribution) is analyzed by the MCA to create a CRT spectrum. This spectrum statistically displays the time fluctuation of the signals that enter the TAC. This fluctuation mainly results from the TTS of the two photomultiplier tubes. As can be seen from Figures 4-14 and 4-20, the TTS is inversely proportional to the square root of the number of photoelectrons per pulse and also to the square root of the supply voltage. In general, therefore, the higher the radiation energy and the supply voltage, the better the CRT will be. If the TTS of each photomultiplier tube is τ_1 and τ_2, the CRT is given by

$$C.R.T. = (\tau_1^2+\tau_2^2)^{1/2} \quad \cdots\cdots \text{(Eq. 4- 10)}$$

The CRT characteristic is an important parameter for TOF measurements because it affects the position resolution.

4.3.2 Linearity

The photomultiplier tube exhibits good linearity[1) 24) 27) 28)] in anode output current over a wide range of incident light levels as well as the photon counting region. In other words, it offers a wide dynamic range. However, if the incident light amount is too large, the output begins to deviate from the ideal linearity. This is primarily caused by anode linearity characteristics, but it may also be affected by cathode linearity characteristics when a photomultiplier tube with a transmission mode photocathode is operated at a low supply voltage and large current. Both cathode and anode linearity characteristics are dependent only on the current value if the supply voltage is constant, while being independent of the incident light wavelength.

(1) Cathode linearity

Photocathode Materials	Spectral Response [Peak Wavelength] (nm)	Upper Limit of Linearity (Average Current)
Ag-O-Cs	300 to1200 [800]	1μA
Sb-Cs	up to 650 [440]	1μA
Sb-Rb-Cs	up to 650 [420]	0.1μA
Sb-K-Cs	up to 650 [420]	0.01μA
Sb-Na-K	up to 650 [375]	10μA
Sb-Na-K-Cs	up to 850 [420], up to 900 [600] extended red	10μA
Ga-As(Cs)	up to 930 [300~700]	(*) 0.1μA
Cs-Te	up to 320 [210]	0.1μA
Cs-I	up to 200 [140]	0.1μA

(*) Linearity considerably degrades if this current is exceeded.

Table 4-4: Photocathode materials and cathode linearity limits

The photocathode is a semiconductor and its electrical resistance depends on the photocathode materials. Therefore, the cathode linearity also differs depending on the photocathode materials as listed in Table 4-4. It should be noted that Table 4-4 shows characteristics only for transmission mode photocathodes. In the case of reflection mode photocathodes which are formed on a metal plate and thus have a sufficiently low resistivity, the linearity will not be a significant problem. To reduce the effects of photocathode resistivity on the device linearity without degrading the collection efficiency, it is recommended to apply a voltage of 50 to 300 volts between the photocathode and the first dynode, depending on the structure. For semiconductors, the photocathode surface resistivity increases as the temperature decreases. Thus, consideration must be given to the temperature characteristics of the photocathode resistivity when cooling the photomultiplier tube.

(2) Anode linearity

The anode linearity is limited by two factors: the voltage-divider circuit and space charge effects due to a large current flowing in the dynodes.

As shown below, the linearity in DC mode operation is mainly limited by the voltage-divider circuit, while the pulse mode operation is limited by space charge effects.

Linearity
- Pulse mode : Limited by the space charge effects.
- DC mode : Limited by a change in the voltage-divider voltage due to the magnitude of signal current.

The linearity limit defined by the voltage-divider circuit is described in Chapter 5. The pulse linearity in pulse mode is chiefly dependent on the peak signal current. When an intense light pulse enters a photomultiplier tube a large current flows in the latter dynode stages, increasing the space charge density, and causing current saturation. The extent of these effects depends on the dynode structure, as indicated in Table 4-2. The space charge effects also depend on the electric field distribution and intensity between each dynode. The mesh type dynodes offer superior linearity because they have a structure resistant to the space charge effects. Each dynode is arranged in close proximity providing a higher electric field strength and the dynode area is large so that the signal density per unit area is lower. In general, any dynode type provides better pulse linearity when the supply voltage is increased, or in other words, when the electric field strength between each dynode is enhanced.

Figure 4-23 shows the relationship between the pulse linearity and the supply voltage of a Hamamatsu photomultiplier tube R2059. The linearity can be improved by use of a special voltage-divider (called "a tapered voltage-divider") designed to increase the interstage voltages at the latter dynode stages. This is described in Chapter 5. Because such a tapered voltage-divider must have an optimum electric field distribution and intensity that match each dynode, determining the proper voltage distribution ratio is a rather complicated operation.

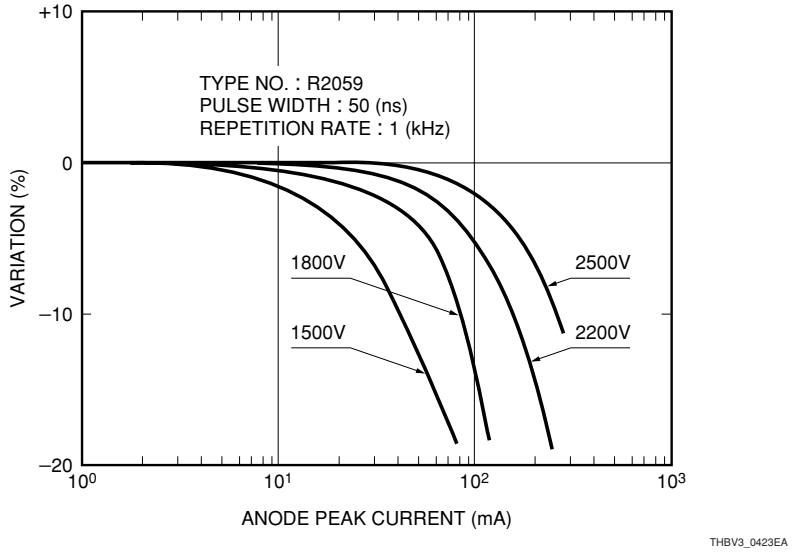

Figure 4-23: Voltage dependence of linearity

(3) Linearity measurement

The linearity measurement methods include the DC mode and the pulse mode. Each mode is described below.

(a) DC mode

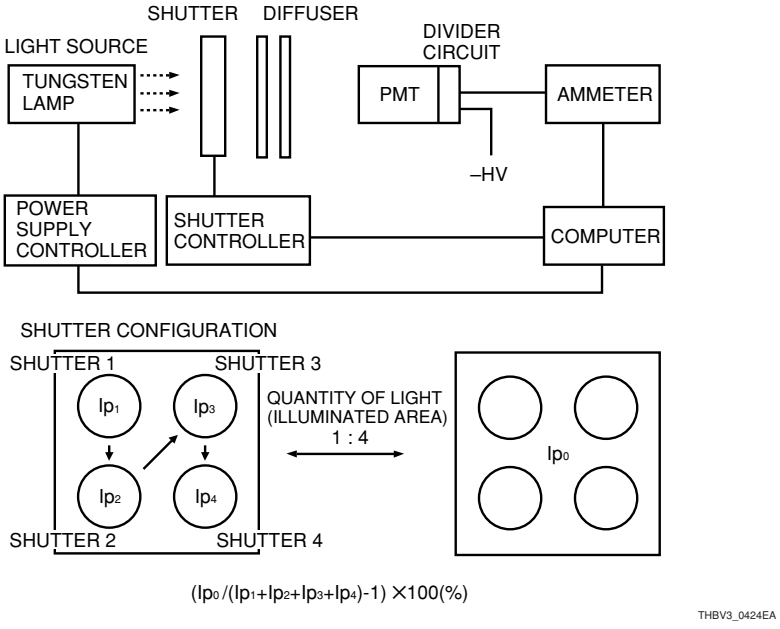

Figure 4-24: Block diagram for DC mode linearity measurement

This section introduces the DC linearity measurement method used by Hamamatsu Photonics. As Figure 4-24 shows, a 4-aperture plate equipped with shutters is installed between the light source and the photomultiplier tube. Each aperture is opened in the order of 1, 2, 3 and 4, finally all four apertures are opened, and the photomultiplier tube outputs are measured (as Ip_1, Ip_2, Ip_3, Ip_4 and Ip_0, respectively). Then the ratio of Ip_0 to (Ip_1+Ip_2+Ip_3+Ip_4) is calculated as follows:

$$(Ip_0/(Ip_1+Ip_2+Ip_3+Ip_4)-1)\times 100(\%) \quad \cdots\cdots \text{(Eq. 4-11)}$$

This value represents a deviation from linearity and if the output is within the linearity range, Ip0 becomes

$$Ip_0 = Ip_1+Ip_2+Ip_3+Ip_4 \quad \cdots\cdots \text{(Eq. 4-12)}$$

Repeating this measurement by changing the intensity of the light source (i.e. changing the photomultiplier tube output current) gives a plot as shown in Figure 4-25. This indicates an output deviation from linearity. This linearity measurement greatly depends on the magnitude of the current flowing through the voltage-divider circuit and its structure.

As a simple method, linearity can also be measured using neutral density filters which are calibrated in advance for changes in the incident light level.

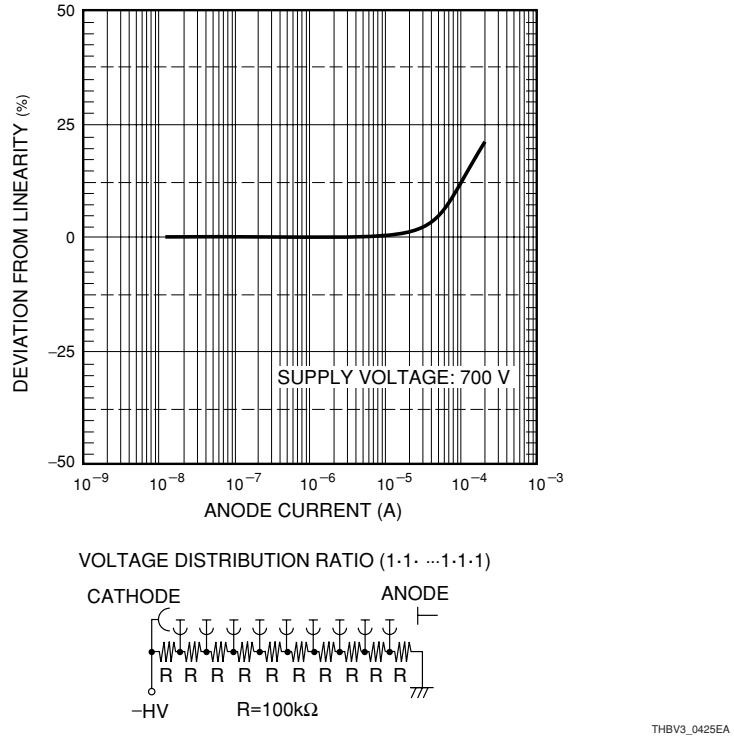

Figure 4-25: DC linearity (side-on type)

(b) Pulse mode

A simplified block diagram for the pulse mode linearity measurement is shown in Figure 4-26. In this measurement, an LED operated in a double-pulsed mode is used to provide higher and lower pulse amplitudes alternately. The higher and lower pulse amplitudes are fixed at a ratio of approximately 4:1. If the photomultiplier tube outputs in response to the higher and lower pulsed light at sufficiently low light levels, the peak currents are Ip_{01} and Ip_{02} respectively, then the ratio of Ip_{02}/Ip_{01} is proportional to the pulse amplitude; thus

$$Ip_{02}/Ip_{01} = 4 \quad \cdots\cdots \text{(Eq. 4-13)}$$

When the LED light sources are brought close to the photomultiplier tube (See Figure 4-26.) and the subsequent output current increases, the photomultiplier tube output begins to deviate from linearity. If the output for the lower pulsed light (A_1) is Ip1 and the output for the higher pulsed light (A_2) is Ip_2, the ratio between the two output pulses has the following relation:

$$Ip_2/Ip_1 \neq Ip_{02}/Ip_{01} \quad \cdots\cdots \text{(Eq. 4-14)}$$

Linearity can be measured by measuring the ratio between the two outputs of the photomultiplier tube, produced by the two different intensities of pulsed light, Ip_2/Ip_1. Linearity is then calculated as follows:

$$\frac{(Ip_2/Ip_1)-(Ip_{02}/Ip_{01})}{(Ip_{02}/Ip_{01})} \times 100\ (\%) \quad \cdots\cdots \text{(Eq. 4-15)}$$

This indicates the extent of deviation from linearity at the anode output Ip_2. If the anode output is in the linearity range, the following relation is always established:

$$(Ip_2/Ip_1) = (Ip_{02}/Ip_{01}) \quad \cdots\cdots \text{(Eq. 4-16)}$$

Under these conditions, Eq. 4-15 becomes zero.

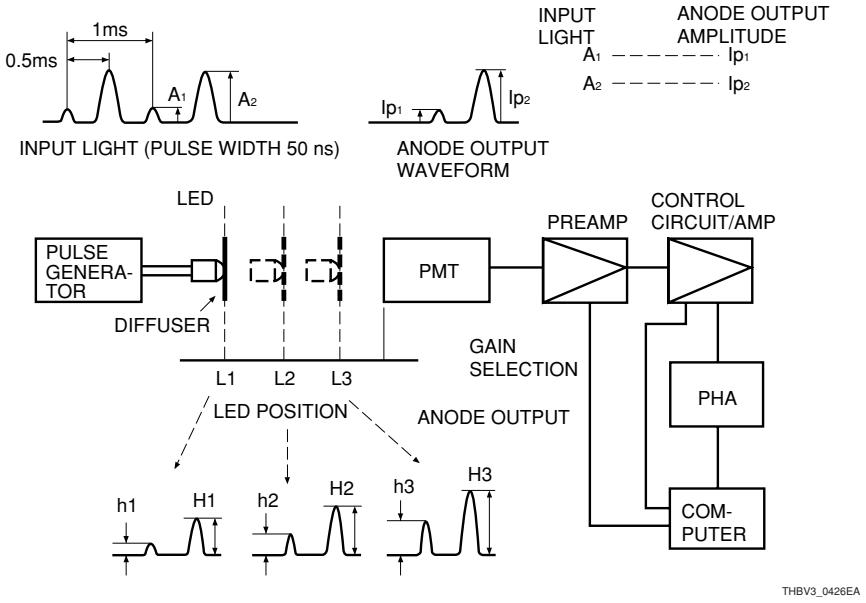

Figure 4-26: Block diagram for pulse mode linearity measurement

By repeating this measurement while varying the distance between the LED light source and the photomultiplier tube so as to change the output current of the photomultiplier tube, linearity curves like those shown in Figure 4-27 can be obtained.

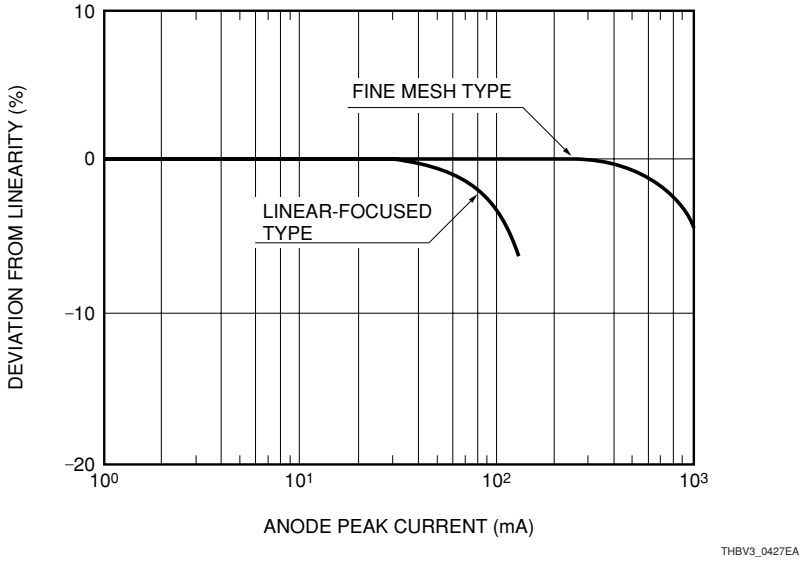

Figure 4-27: Pulse linearity

4.3.3 Uniformity

Uniformity is the variation of the output signal with respect to the photocathode position. Anode output uniformity is thought to be the product of the photocathode uniformity and the electron multiplier (dynode section) uniformity.

Figure 4-28 shows anode uniformity data measured at wavelengths of 400 nanometers and 800 nanometers. This data is obtained with a light spot of 1 mm diameter scanned over the photocathode surface.

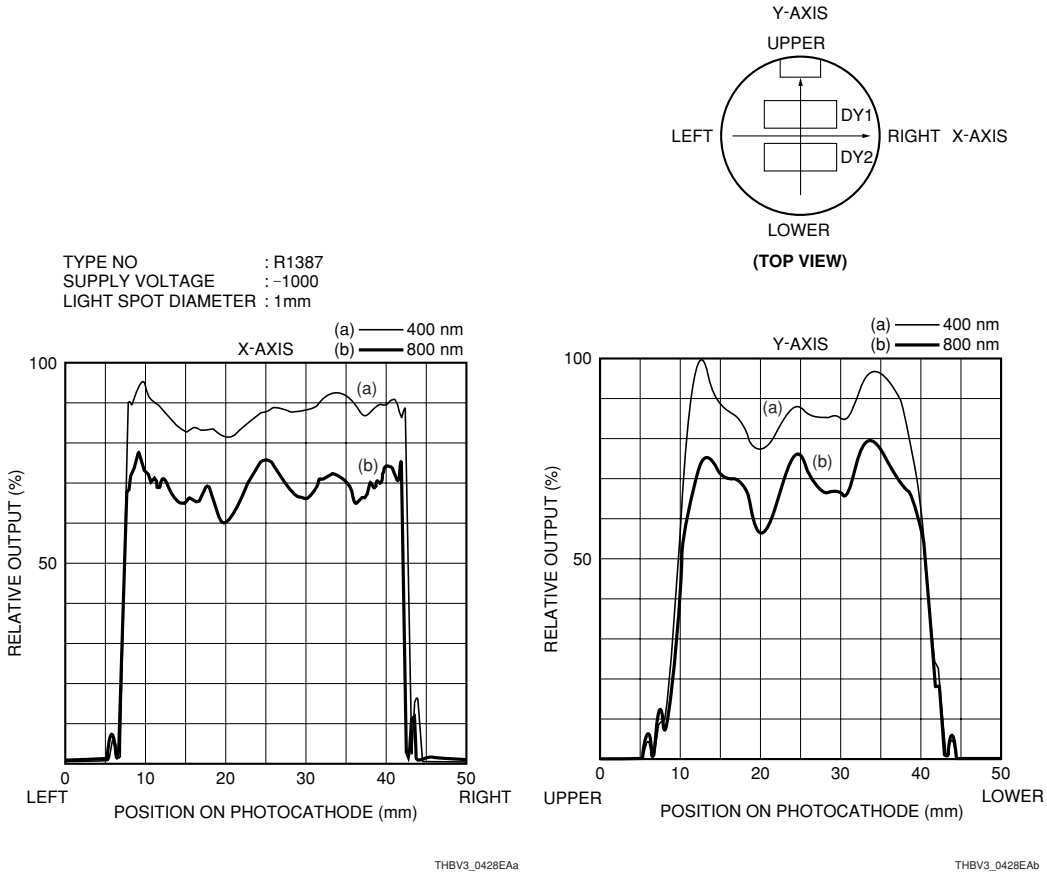

Figure 4-28: Difference in uniformity with wavelength

In general, both photocathode uniformity and anode uniformity deteriorate as the incident light shifts to a longer wavelength, and especially as it approaches the long-wavelength limit. This is because the cathode sensitivity near the long-wavelength limit greatly depends on the surface conditions of the photocathode and thus fluctuations increase. Moreover, if the supply voltage is too low, the electron collection efficiency between dynodes may degrade and adversely affect uniformity.

Head-on photomultiplier tubes provide better uniformity in comparison with side-on types. In such applications as gamma cameras used for medical diagnosis where good position detecting ability is demanded, uniformity is an important parameter in determining equipment performance. Therefore, the photomultiplier tubes used in this field are specially designed and selected for better uniformity. Figure 4-29 shows typical uniformity data for a side-on tube. The same measurement procedure as for head-on tubes is used. Uniformity is also affected by the dynode structure. As can be seen from Table 4-2, the box-and-grid type, venetian blind type and mesh type offer better uniformity.

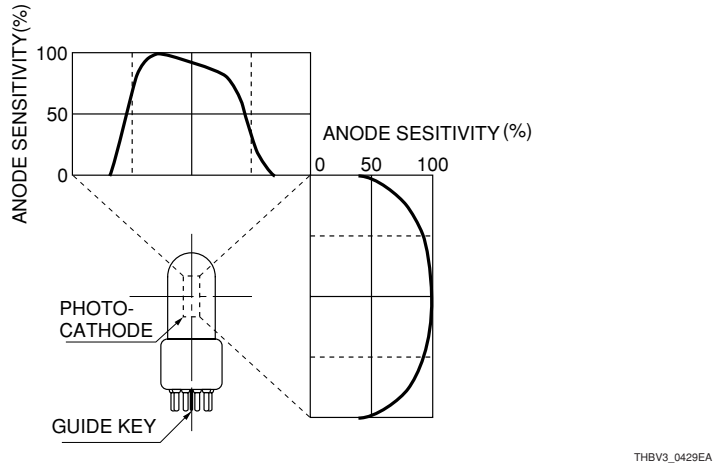

Figure 4-29: Uniformity of a side-on photomultiplier tube

Considering actual photomultiplier tube usage, uniformity is evaluated by two methods: one measured with respect to the position of incidence (spatial uniformity) and one with respect to the angle of incidence (angular response). The following sections explain their measurement procedures and typical characteristics.

(1) Spatial uniformity

To measure spatial uniformity, a light spot is scanned in two-dimensions over the photocathode of a photomultiplier tube and the variation in output current is graphically displayed. Figure 4-30 shows a schematic diagram for the spatial uniformity measurement.

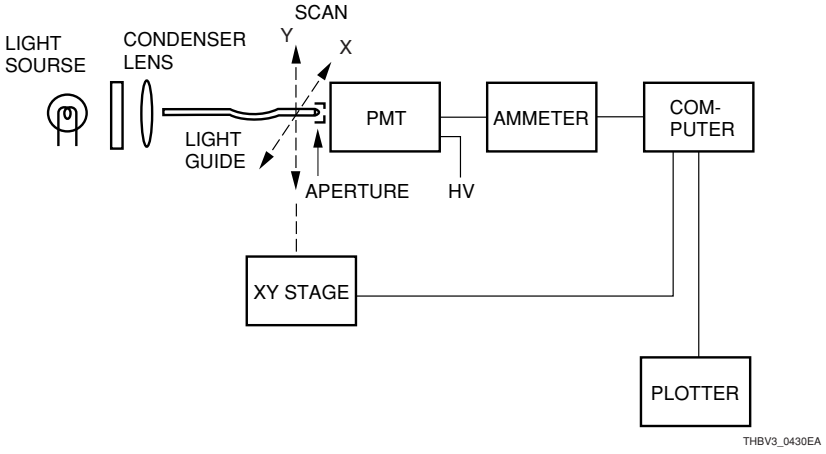

Figure 4-30: Schematic diagram for spatial uniformity measurement

For convenience, the photocathode is scanned along the X-axis and Y-axis. The direction of the X-axis or Y-axis is determined with respect to the orientation of the first dynode as shown in Figure 4-31.

Figure 4-31 also shows the position relation between the XY axes and the first dynode. The degree of loss of electrons in the dynode section significantly depends on the position of the first dynode on which the photoelectrons strike. Refer to Figure 4-28 for specific uniformity data.

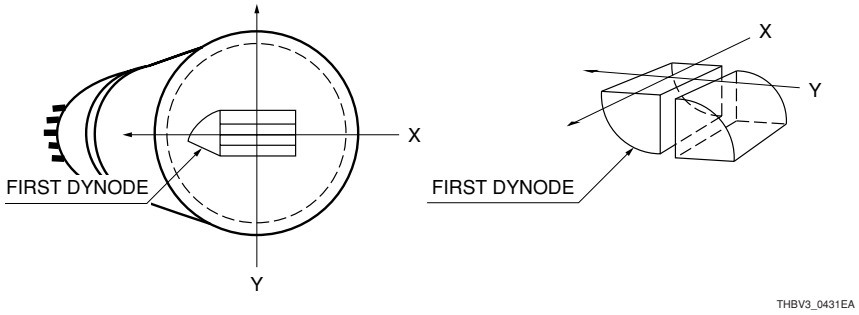

Figure 4-31: Spatial uniformity measurement for head-on types

While the photocathode is scanned by the light spot, the emitted photoelectrons travel along the X-axis or Y-axis of the first dynode as shown in Figure 4-32.

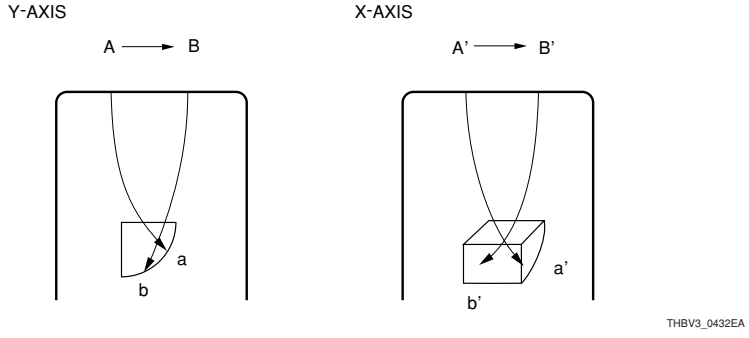

Figure 4-32: Position of photoemission and the related position on the first dynode

This method for measuring spatial uniformity is most widely used because the collective characteristics can be evaluated in a short time. In some cases, spatial uniformity is measured by dividing the photocathode into a grid pattern, so that sensitivity distribution is displayed in two or three dimensions.

The spatial uniformity of anode output ranges from 20 to 40 percent for head-on tubes, and may exceed those values for side-on tubes. The adverse effects of the spatial uniformity can be minimized by placing a diffuser in front of the input window of a photomultiplier tube or by using a photomultiplier tube with a frosted glass window.

(2) Angular response

Photomultiplier tube sensitivity somewhat depends on the angle of incident light on the photocathode. This dependence on the incident angle is called the angular response.[28)-30)] To measure the angular response, the entire photocathode is illuminated with collimated light, and the output current is measured while rotating the photomultiplier tube. A schematic diagram for the angular response measurement is shown in Figure 4-33 and specific data is plotted in Figure 4-34. As the rotary table is rotated, the projected area of the photocathode is reduced. This means that the output current of a photomultiplier tube is plotted as a cosine curve of the incident angle even if the output has no dependence on the incident angle. Commonly, the photocathode sensitivity improves at larger angles of incidence and thus the output current is plotted along a curve showing higher sensitivity than the cosine (cos θ) curve. This is because the incident light transmits across a longer distance at large angles of incidence. In addition, this increase in sensitivity usually becomes larger at longer wavelengths.

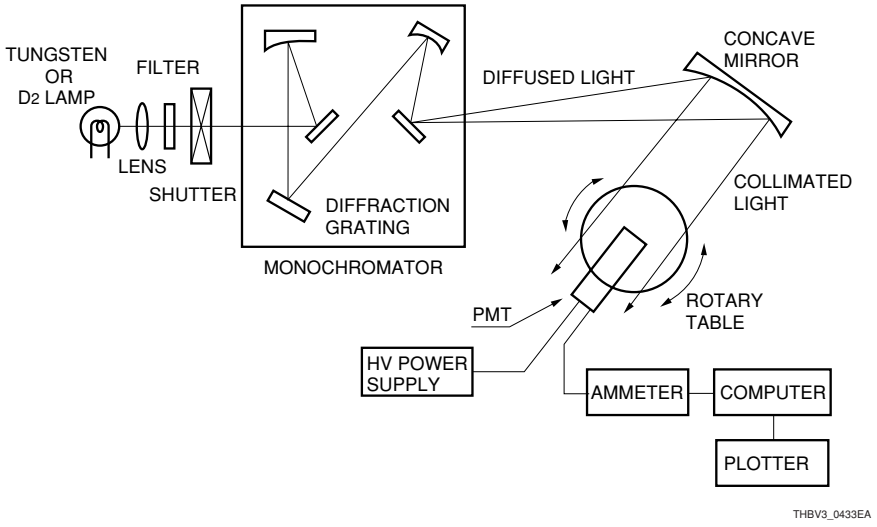

Figure 4-33: Schematic diagram for angular response measurement

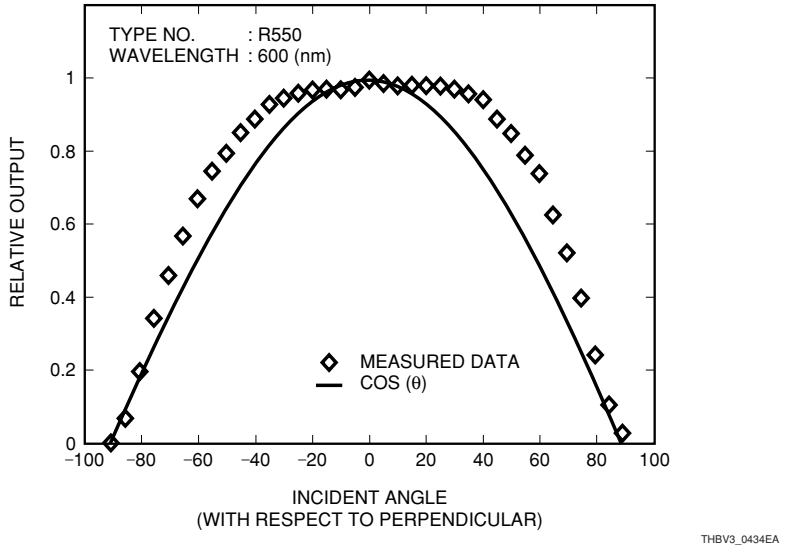

Figure 4-34: Typical angular response

4.3.4 Stability

The output variation of a photomultiplier tube with operating time is commonly termed as "drift" or "life" characteristics. On the other hand, the performance deterioration resulting from the stress imposed by the supply voltage, current, and ambient temperature is called "fatigue".

(1) Drift (time stability) and life characteristics

Variations (instability) over short time periods are mainly referred to as drift[1) 31)], while variations (instability) over spans of time longer than 10^3 to 10^4 hours are referred to as the life characteristics. Since the cathode sensitivity of a photomultiplier tube exhibits good stability even after long periods of operating time, the drift and life characteristics primarily depend on variations in the secondary emission ratio. In other words, these characteristics indicate the extent of gain variation with operating time.

Drift per unit time generally improves with longer operating time and this tendency continues even if the photomultiplier tube is left unused for a short time after operation. Aging or applying the power supply voltage to the photomultiplier tube prior to use ensures more stable operation.

Since drift and life characteristics greatly depend on the magnitude of signal output current, keeping the average output current within a few microamperes is usually recommended.

At Hamamatsu Photonics, drift is usually measured in the DC mode by illuminating a photomultiplier tube with a continuous light and recording the output current with the operating time. Figure 4-35 shows specific drift data for typical Hamamatsu photomultiplier tubes. In most cases, the drift of a photomultiplier tube tends to vary largely during initial operation and stabilizes as operating time elapses. In pulsed or intermittent operation (cyclic on/off operation), the drift shows a variation pattern similar to those obtained with continuous light if the average output current is of the same level as the output current in the DC mode.

In addition, there are other methods for evaluating the drift and life characteristics, which are chiefly used for photomultiplier tubes designed for scintillation counting. For more details refer to Chapter 7, "Scintillation counting".

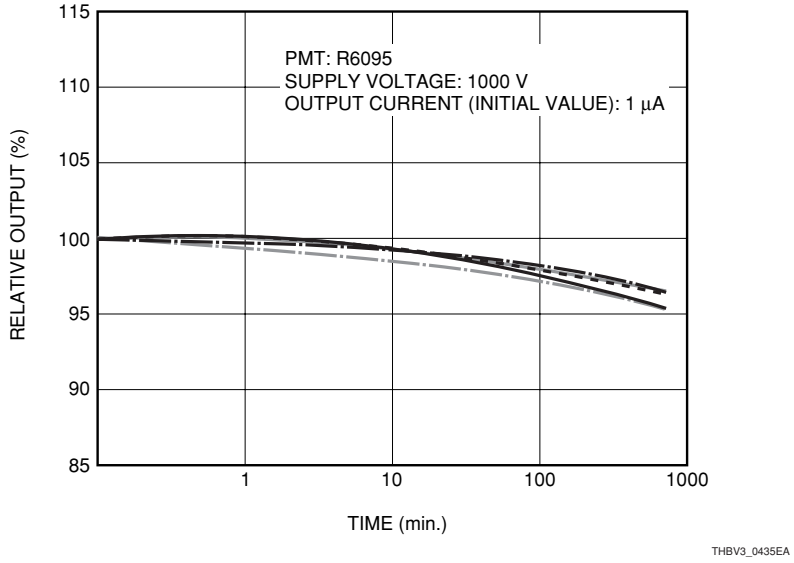

Figure 4-35: Examples of drift data

(2) Aging and warm-up

In applications where output stability within a few percent is required, aging or warm-up is recommended as explained below.

(a) Aging

Aging is a technique in which a photomultiplier tube is continuously operated for a period ranging from several hours to several tens of hours, with the anode output current not exceeding the maximum rating. Through this aging, drift can be effectively stabilized. In addition, if the photomultiplier tube is warmed up just before actual use, the drift will be further stabilized.

(b) Warm-up

For stable operation of a photomultiplier tube, warm-up of the photomultiplier tube for about 30 to 60 minutes is recommended. The warm-up period should be longer at the initial phase of photomultiplier tube operation, particularly in intermittent operation. After a long period of operation warm-up can be shortened. At a higher anode current the warm-up period can be shortened and at a lower anode current the warm-up should be longer. In most cases, a warm-up is performed for several ten minutes at a supply voltage near the actual operating voltage and an anode current of several microamperes. However, in low current operation (average output current from less than one hundred up to several hundred nanoamperes), a warm-up is done by just applying a voltage to the photomultiplier tube for about one hour in the dark state.

4.3.5 Hysteresis

When the incident light or the supply voltage is changed in a step function, a photomultiplier tube may not produce an output comparable with the same step function. This phenomenon is known as "hysteresis".[1) 32)] Hysteresis is observed as two behaviors: "overshoot" in which the output current first increases greatly and then settles and "undershoot" in which the output current first decreases and then returns to a steady level. Hysteresis is further classified into "light hysteresis" and "voltage hysteresis" depending on the measurement conditions. Some photomultiplier tubes have been designed to suppress hysteresis by coating the insulator surface of the electrode supports with a conductive material so as to minimize the electrostatic charge on the electrode supports without impairing their insulating properties.

(1) Light hysteresis

When a photomultiplier tube is operated at a constant voltage, it may exhibit a temporary variation in the anode output after the incident light is changed in a step function. This variation is called light hysteresis. Figure 4-36 shows the Hamamatsu test method for light hysteresis and typical hysteresis waveforms.

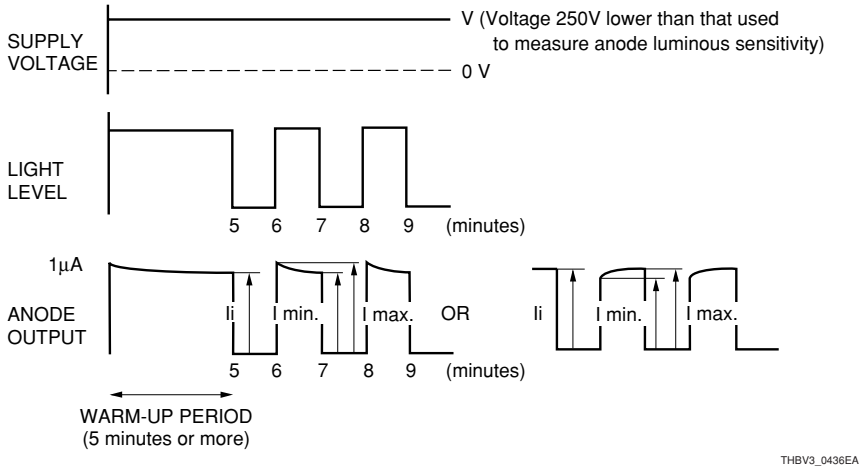

Figure 4-36: Light hysteresis

As shown in Figure 4-36, a photomultiplier tube is operated at a voltage V, which is 250 volts lower than the voltage used to measure the anode luminous sensitivity. The photomultiplier tube is warmed up for five minutes or more at a light level producing an anode current of approximately 1 microampere. Then the incident light is shut off for one minute and then input again for one minute. This procedure is repeated twice to confirm the reproducibility. By measuring the variations of the anode outputs, the extent of light hysteresis can be expressed in percent, as follows:

$$\text{Light hysteresis } H_L = ((I_{MAX}-I_{MIN})/Ii)\times 100(\%) \quad \cdots\cdots \text{(Eq. 4-17)}$$

where I_{MAX} is the maximum output value, I_{MIN} is the minimum output value and Ii is the initial output value.

Table 4-5 shows typical hysteresis data for major Hamamatsu photomultiplier tubes. Since most photomultiplier tubes have been designed to minimize hysteresis, they usually only display a slight hysteresis within ±1 percent. It should be noted that light hysteresis behaves in different patterns or values, depending on the magnitude of the output current.

(2) Voltage hysteresis

When the incident light level cycles in a step function, the photomultiplier tube is sometimes operated with a feedback circuit that changes the supply voltage in a complimentary step function so that the photomultiplier tube output is kept constant. In this case, the photomultiplier tube output may overshoot or undershoot immediately after the supply voltage is changed. This phenomenon is called voltage hysteresis and should be suppressed to the minimum possible value. Generally, this voltage hysteresis is larger than light hysteresis and even tubes with small light hysteresis may possibly exhibit large voltage hysteresis. Refer to Table 4-5 below for typical hysteresis data.

PMT	Light Hysteresis H_L (%)	Voltage Hysteresis Hv (%)	Tube Diameter (mm)
R6350	0.3	0.5	13mm side-on
R212	0.2	1.0	28mm side-on
R928	0.1	1.0	28mm side-on
R647	0.9	2.5	13mm head-on
R6095	0.4	2.0	28mm head-on
R1306	0.07	0.06	52mm head-on

Table 4-5: Typical hysteresis data for major Hamamatsu photomultiplier tubes

Figure 4-37 shows a procedure for measuring voltage hysteresis. A photomultiplier tube is operated at a voltage V, which is 700 volts lower than the voltage used to measure the anode luminous sensitivity. The tube is warmed up for five minutes or more at a light level producing an anode current of approximately 0.1 microamperes.

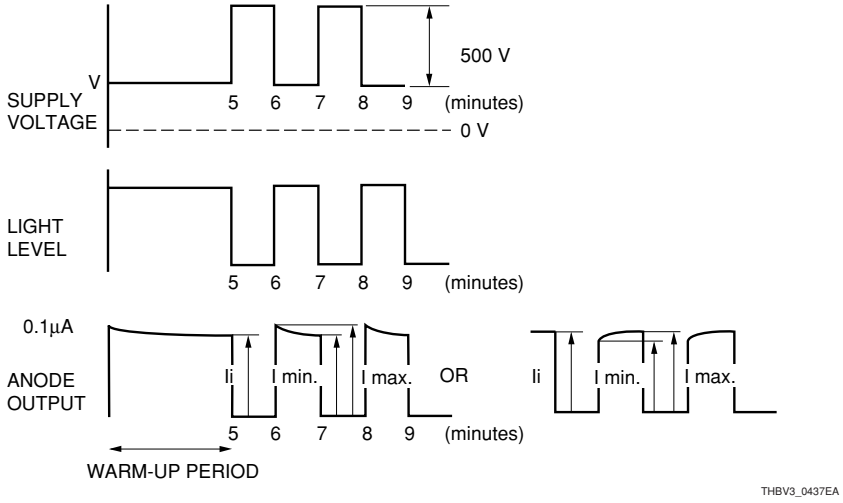

Figure 4-37: Voltage hysteresis

Then the incident light is shut off for one minute while the supply voltage is increased in 500 volt step. Then the light level and supply voltage are returned to the original conditions. This procedure is repeated to confirm the reproducibility. By measuring the variations in the anode outputs, the extent of voltage hysteresis is expressed in percent, as shown in Eq. 4-8 below. In general, the higher the change in the supply voltage, the larger the voltage hysteresis will be. Other characteristics are the same as those for light hysteresis.

$$\text{Voltage hysteresis } H_V = ((I_{MAX}-I_{MIN})/Ii)\times 100(\%) \cdots\cdots\cdots\cdots \text{(Eq. 4-18)}$$

where I_{MAX} is the maximum output value, I_{MIN} is the minimum output value and Ii is the initial output value.

(3) Reducing the hysteresis

When a signal light is blocked for a long period of time, applying a dummy light to the photomultiplier tube to minimize the change in the anode output current is effective in reducing the possible light hysteresis. Voltage hysteresis may be improved by use of HA coating. (Refer to section 8.2 in Chapter 13.)

4.3.6 Dark current

A small amount of current flows in a photomultiplier tube even when operated in a completely dark state. This output current is called the dark current[1) 23) 25) 33)] and ideally it should be kept as small as possible because photomultiplier tubes are used for detecting minute amounts of light and current.

(1) Causes of dark current

Dark current may be categorized by cause as follows:

(a) Thermionic emission current from the photocathode and dynodes

(b) Leakage current (ohmic leakage) between the anode and other electrodes inside the tube and/or between the anode pin and other pins on the bulb stem

(c) Photocurrent produced by scintillation from glass envelope or electrode supports

(d) Field emission current

(e) Ionization current from residual gases (ion feedback)

(f) Noise current caused by cosmic rays, radiation from radioisotopes contained in the glass envelopes and environmental gamma rays

Dark current increases with an increasing supply voltage, but the rate of increase is not constant. Figure 4-38 shows a typical dark current vs. supply voltage characteristic.

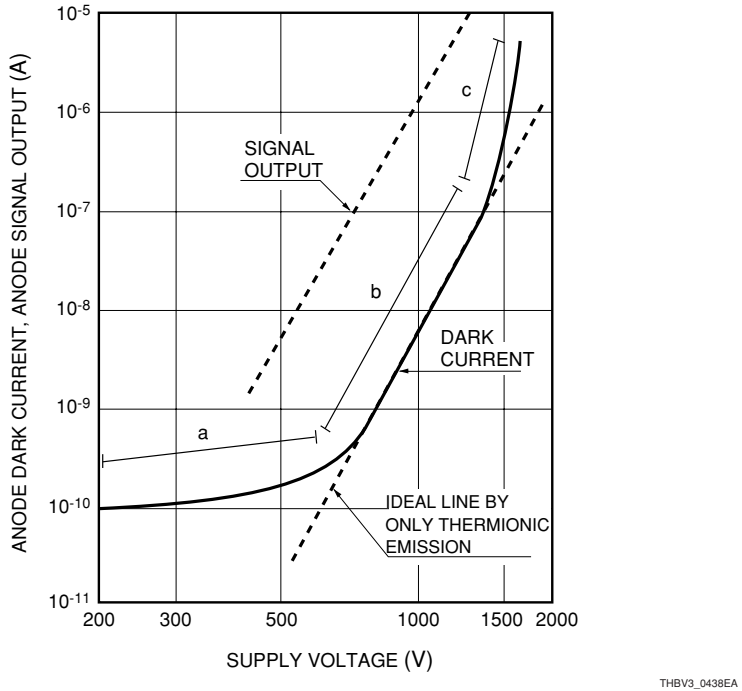

Figure 4-38: Typical dark current vs. supply voltage characteristic

This characteristic is related to three regions of the supply voltage: a low voltage region (a in Figure 4-38), a medium voltage region (b in Figure 4-38), and a high voltage region (c in Figure 4-38). Region a is dominated by the leakage current, region b by the thermionic emission, and region c by the field emission and glass or electrode support scintillation. In general, region b provides the best signal-to-noise ratio, so operating the photomultiplier tube in this region would prove ideal.

Ion feedback[34] and noise[34) 35) 36)] originating from cosmic rays and radioisotopes will sometimes be a problem in pulse operation.

When a photocathode is exposed to room illumination, the dark current will return to the original level by storing the photomultiplier tube in a dark state for one to two hours. However, if exposed to sunlight or extremely intense light (10,000 lux or higher), this may cause unrecoverable damage and must therefore be avoided. It is recommended to store the photomultiplier tube in a dark state before use.

The dark current data furnished with Hamamatsu photomultiplier tubes is measured after the tube has been stored in a dark state for 30 minutes. This "30-minute storage in a dark state" condition allows most photomultiplier tubes to approach the average dark current level attained after being stored for a long period in a dark state. This is also selected in consideration of the work efficiency associated with measuring the dark current. If the tube is stored for a greater length of time in a dark state, the dark current will decrease further. The following sections explain each of the six causes of dark current listed above.

a) Thermionic emission

Since the photocathode and dynode surfaces are composed of materials with a very low work function, they emit thermionic electrons even at room temperatures. This effect has been studied by W. Richardson, and is stated by the following equation.[37)]

$$i_s = AT^{5/4}e^{(-e\psi/KT)} \quad \text{(Eq. 4-19)}$$

where,

ψ : work function
T : absolute temperature
e : electron charge
A : constant
K : Boltzmann constant

It can be seen from this equation that thermionic emission is a function of the photocathode work function and absolute temperature. Thus the magnitude of the work function as well as the photocathode material govern the amount of thermionic emission. When the photocathode work function is low, the spectral response extends to the light with lower energy or longer wavelengths, but with an increase in the thermionic emission. Among generally used photocathodes composed of alkali metals, the Ag-O-Cs photocathode with a spectral response in the longest wavelength range (see Figure 4-2) exhibits the highest dark current. In contrast, the photocathodes for the ultraviolet range (Cs-Te, Cs-I) exhibit the shortest wavelength upper limit and provide the lowest dark current.

Eq. 4-19 also implies that the dark current decreases with decreasing temperature. Therefore, as shown in Figure 4-39, cooling a photomultiplier tube is an effective technique for reducing the dark current.

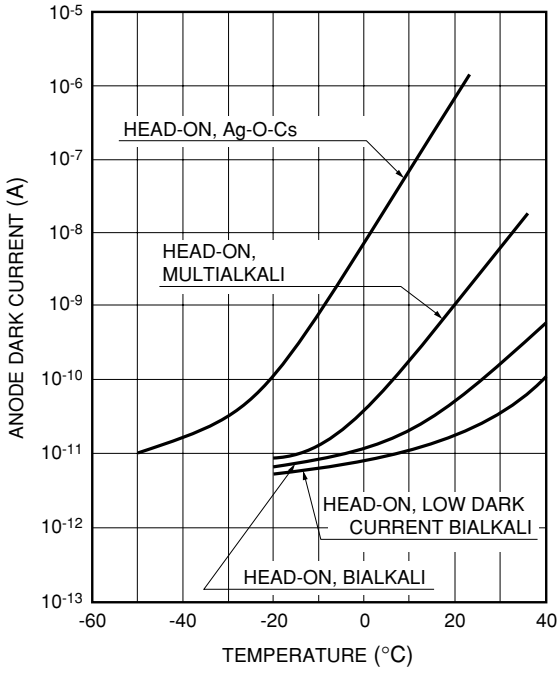

Figure 4-39: Temperature characteristics of anode dark current

However, when the dark current reduces down to a level where the leakage current predominates, this effect becomes limited. Although thermionic emission occurs both from the photocathode and the dynodes, the thermionic emission from the photocathode has a much larger effect on the dark current. This is because the photocathode is larger than each dynode in size and also because the dynodes, especially at the latter stages, contribute less to the output current. Consequently, the dark current caused by the thermionic emission vs. the supply voltage characteristic will be nearly identical with the slope of gain vs. supply voltage.

Figure 4-40 describes temperature characteristics for dark pulses measured in the photon counting method. In this case as well, the number of dark pulses is decreased by cooling the photocathode.

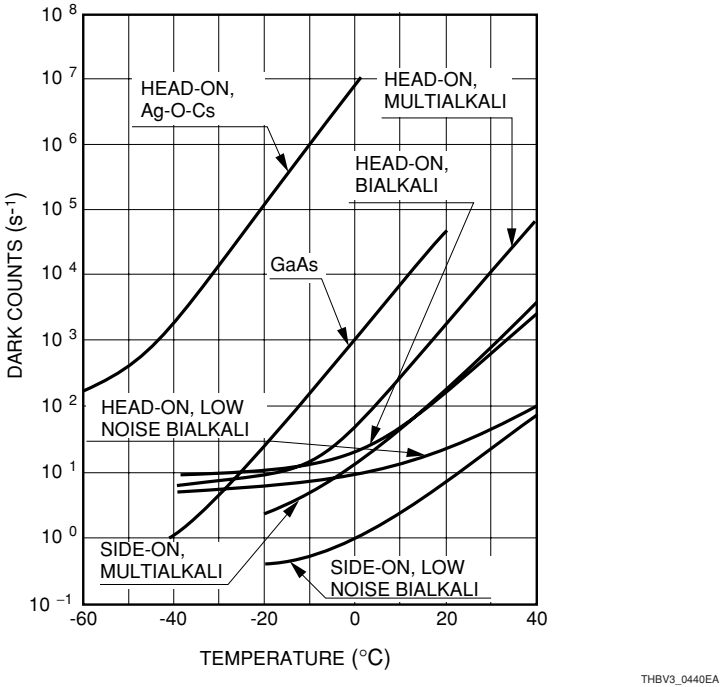

Figure 4-40: Temperature characteristics for dark current pulse

b) Leakage current (ohmic leakage)

Photomultiplier tubes are operated at high voltages from 500 up to 3000 volts, but they handle very low currents from several nanoamperes to less than 100 microamperes. Therefore, the quality of the insulating materials used in the tubes is very important. For instance, if the insulation resistance is around 10^{12} ohms, the leakage current may reach the nanoampere level. The relationship between the leakage current from the insulating materials and the supply voltage is determined by Ohm's law, i.e., current value (I) = supply voltage (V)/insulation resistance (R), regardless of the gain of the photomultiplier tube as seen in Figure 4-38. On the other hand, the dark current resulting from thermionic emission varies exponentially with the supply voltage. Thus, as mentioned in the previous section, the leakage current has relatively more effect on the dark current as the supply voltage is lowered.

A leakage current may be generated between the anode and the last dynode inside a tube. It may also be caused by imperfect insulation of the glass stem and base, and between the socket anode pin and other pins. Since contamination from dirt and moisture on the surface of the glass stem, base, or socket increases the leakage current, care should be taken to keep these parts clean and at low humidity. If contaminated, they can be cleaned with alcohol in most cases. This is effective in reducing the leakage current.

c) Scintillation from the glass envelope or electrode support materials

Some electrons emitted from the photocathode or dynodes may deviate from their normal trajectories and do not contribute to the output signal. If these stray electrons impinge on the glass envelope, scintillations may occur and result in dark pulses. In general, a photomultiplier tube is operated with a negative high voltage applied to the photocathode and is housed in a metal case at ground potential. This arrangement tends to cause stray electrons to impinge on the glass envelope. However, this problem can be minimized by using a technique called "HA coating". Refer to section 8.2 in Chapter 13 for detailed information on HA coating.

d) Field emission

If a photomultiplier tube is operated at an excessive voltage, electrons may be emitted from the dynodes by the strong electric field. Subsequently the dark current increases abruptly. This phenomenon occurs in region c in Figure 4-38 and shortens the life of the photomultiplier tube considerably. Therefore, the maximum supply voltage is specified for each tube type and must be observed. As long as a photomultiplier tube is operated within this maximum rating there will be no problem. But for safety, operating the photomultiplier tube at a voltage 20 to 30 percent lower than the maximum rating is recommended.

e) Ionization current of residual gases (ion feedback)

The interior of a photomultiplier tube is kept at a vacuum as high as 10^{-6} to 10^{-5} Pa. Even so, there exist residual gases that cannot be ignored. The molecules of these residual gases may be ionized by collisions with electrons. The positive ions that strike the front stage dynodes or the photocathode produce many secondary electrons, resulting in a large noise pulse. During high current operation, this noise pulse is usually identified as an output pulse appearing slightly after the main photocurrent. This noise pulse is therefore called an afterpulse[38) 39) 40)] and may cause a measurement error during pulsed operation.

f) Noise current caused by cosmic rays, radiation from radioisotopes contained in the glass envelopes and environmental gamma rays

Many types of cosmic rays are always falling on the earth. Among them, muons (μ) can be a major source of photomultiplier tube noise. When muons pass through the glass envelope, Cherenkov radiation may occur, releasing a large number of photons. In addition, most glasses contain potassium oxide (K_2O) which also contains a minute amount of the radioactive element ^{40}K. ^{40}K emits beta and gamma rays which may cause noise. Furthermore, environmental gamma rays emitted from radioisotopes contained in buildings may be another noise source. However, because these dark noises occur much less frequently, they are negligible except for applications such as liquid scintillation counting where the number of signal counts is exceptionally small.

(2) Expression of dark current

Dark current is a critical factor that governs the lower detection limit in low light level measurements. There are various methods and terms used to express dark current. The following introduces some of them.

a) DC expression

In general, most Hamamatsu photomultiplier tubes are supplied with dark current data measured at a constant voltage. The dark current may be measured at a voltage at which a particular value of anode sensitivity is obtained. In this case, the dark current is expressed in terms of equivalent dark current or EADCI (equivalent anode dark current input). The equivalent dark current is simply the dark current measured at the voltage producing a specific anode luminous sensitivity, and is a convenient parameter when the tube is operated with the anode sensitivity maintained at a constant value. The EADCI is the value of the incident light flux required to produce an anode current equal to the dark current and is represented in units of lumens or watts as follows:

$$\text{EADCI (lm)} = \text{Dark current (A)} / \text{Anode luminous sensitivity (A/lm)} \cdots\cdots \text{(Eq. 4-20)}$$

When representing the EADCI in watts (W), a specified wavelength is selected and the dark current is divided by the anode radiant sensitivity (A/W) at that wavelength. Figure 4-41 illustrates an example of EADCI data along with the anode dark current and anode luminous sensitivity. A better signal-to-noise ratio can be obtained when the tube is operated in the supply voltage region with a small EADCI. It is obvious from this figure that the supply voltage region in the vicinity of 1000 volts displays a small, flat EADCI curve, yet offers an adequate anode sensitivity of three orders of magnitude.

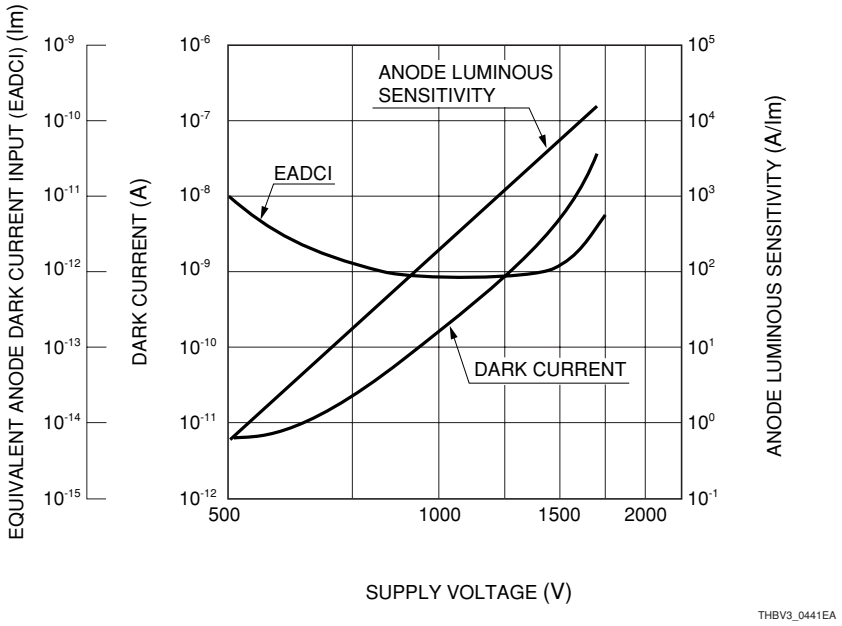

Figure 4-41: Example of EADCI

b) AC expression

In low-level-light measurements, the DC components of dark current can be subtracted. The lower limit of light detection is determined rather by the fluctuating components or noise. In this case, the noise is commonly expressed in terms of ENI (equivalent noise input). The ENI is the value of incident light flux required to produce an output current equal to the noise current, i.e., the incident light level that provides a signal-to-noise ratio of unity. When the ENI is expressed in units of watts (W) at the peak wavelength or at a specific wavelength, it is also referred to as the NEP (noise equivalent power).

Because the noise is proportional to the square root of the circuit bandwidth, the ENI[23] is defined as follows:

$$ENI = (2e \cdot Id \cdot \mu \cdot B)^{1/2}/S \ (W) \quad \cdots\cdots \text{(Eq. 4-21)}$$

where

e: electron charge (1.6×10^{-19} C)
Id: anode dark current (A)
μ: current amplification
B: circuit bandwidth (Hz)
S: anode radiant sensitivity (A/W)

Commonly, Δf=1Hz is used and the ENI value ranges from 10^{-15} to 10^{-16} (W) at the peak wavelength.

4.3.7 Signal-to-noise ratio of photomultiplier tubes

When observing the output waveform of a photomultiplier tube, two types of noise components can be seen: one is present even without light input, and the other is generated by the input of signal light. Normally, these noise components are governed by the dark current generated by the photocathode thermionic emission and the shot noise resulting from the signal current. Both of these noise sources are discussed here.

The signal-to-noise ratio referred to in the following description is expressed in r.m.s. (root mean square). When signal and noise waveforms like those shown in Figure 4-42 are observed, they can be analyzed as follows:

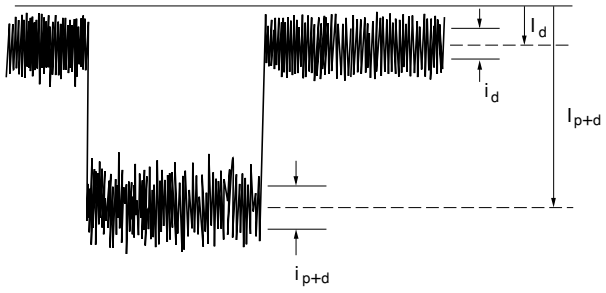

Figure 4-42: Example of signal-to-noise ratio

Mean value of noise component	: I_d
AC component of noise	: i_d (r.m.s.)
Mean value of signal (noise component included)	: I_{p+d}
AC component of signal (noise component included)	: i_{p+d} (r.m.s.)

Using these factors, the signal-to-noise ratio[25) 41) 42)] is given by

$$\text{SN ratio} = I_p/i_{p+d} \quad \cdots\cdots \text{(Eq. 4-22)}$$

where I_p is the mean value of the signal component only, which is obtained by subtracting I_d from I_{p+d}.

If the dark current Id is low enough to be ignored ($I_p >> I_d$), the signal-to-noise ratio will be

$$\text{SN ratio} \approx I_p/i_p \quad \cdots\cdots \text{(Eq. 4-23)}$$

where I_p is the mean value of the signal component and i_p is the AC component (r.m.s.) of the signal. i_p consists of a component associated with the statistical fluctuation of photons and the photoemission process and a component created in the multiplication process. The noise component produced in the multiplication process is commonly expressed in terms of the NF (noise figure)[42)]. The NF indicates how much the signal-to-noise ratio will degrade between the input and output, and is defined as follows:

$$F = (S/N)^2_{in}/(S/N)^2_{out} \quad \cdots\cdots \text{(Eq. 4-24)}$$

where $(S/N)_{in}$ is the signal-to-noise ratio on the photomultiplier tube input side and $(S/N)_{out}$ is the signal-to-noise ratio on the photomultiplier tube output side. With a photomultiplier tube having n dynode stages, the NF from the cascade multiplication process is given by the following equation:

$$F = 1+1/\delta_1+1/\delta_1\delta_2+\cdots+1/\delta_1\delta_2\cdot\cdot\delta_n \quad \cdots\cdots \text{(Eq. 4-25)}$$

where δ_1, δ_2 ... δ_n are the secondary emission ratios at each stage.

With δ_1, δ_2, δ, ...δ_n=δ, Eq. 4-25 is simplified as follows:

$$F \approx \delta/(\delta-1) \quad \text{(Eq. 4-26)}$$

Thus by adding the NF to the AC component i_p, ip is expressed by the following equation:

$$i_p = \mu(2 \cdot e \cdot I_k \cdot \alpha \cdot B \cdot F)^{1/2} \quad \text{(Eq. 4-27)}$$

where α is the collection efficiency, μ is the gain, e is the electron charge, I_k is the cathode current and B is the bandwidth of the measurement system. From this equation and Eq. 4-25, ip becomes

$$i_p = \mu\{2 \cdot e \cdot I_k \cdot \alpha \cdot B(1+1/\delta_1+1/\delta_1\delta_2+\cdots+1/\delta_1\delta_2\cdots\delta_n)\}^{1/2} \quad \text{(Eq. 4-28)}$$

On the other hand, the average anode current I_p is expressed in the following equation:

$$I_p = I_k \cdot \alpha \cdot \mu \quad \text{(Eq. 4-29)}$$

From Eqs. 4-28 and 4-29, the signal-to-noise ratio becomes

$$\text{SN ratio} = I_p/i_p$$
$$= \left(\frac{I_K \alpha}{2eB} \cdot \frac{1}{1+1/\delta_1+1/\delta_1\delta_2+\cdots+1/\delta_1\delta_2\cdots\delta_n}\right)^{1/2}$$

With α = 1 the above equation can be simplified using Eq. 4-26, as follows:

$$\text{SN ratio} \approx \left(\frac{I_K}{2eB} \cdot \frac{1}{\delta/(\delta-1)}\right)^{1/2} \quad \text{(Eq. 4-30)}$$

From this relationship, it is clear that the signal-to-noise ratio is proportional to the square root of the cathode current I_k and is inversely proportional to the square root of the bandwidth B.

To obtain a better signal-to-noise ratio, the shot noise should be minimized and the following points observed:

(1) Use a photomultiplier tube that has as high a quantum efficiency as possible in the wavelength range to be measured.

(2) Design the optical system for better light collection efficiency so that the incident light is guided to the photomultiplier tube with minimum loss.

(3) Use a photomultiplier tube that has an optimum configuration for light collection.

(4) Narrow the bandwidth as much as possible, as long as no problems occur in the measurement system.

By substituting δ = 6 into Eq. 4-30, which is the typical secondary emission ratio of a normal photomultiplier tube, the value $\delta/(\delta-1)$ will be 1.2, a value very close to 1. Consequently, if the noise in the multiplication process is disregarded, the signal-to-noise ratio can be rearranged as follows:

$$\text{SN ratio} = (I_k/2eB)^{1/2} \approx 1.75 \times 10^3 \sqrt{\frac{I_k(\mu A)}{B(MHz)}} \quad \text{(Eq. 4-31)}$$

Figure 4-43 shows the output voltage waveforms obtained while the light level and load resistance are changed under certain conditions. These prove that the relation in Eq. 4-31 is correct.

(a) R_L=20kΩ

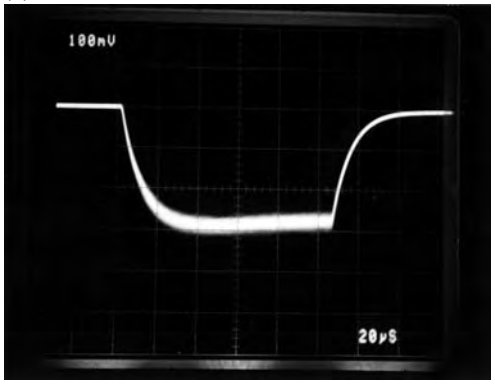

(b) R_L=2kΩ (Bandwidth is 10 times wider than (a))

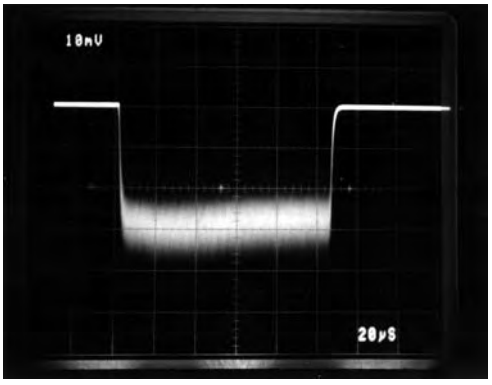

(c) Light level is 10 times higher than (b)

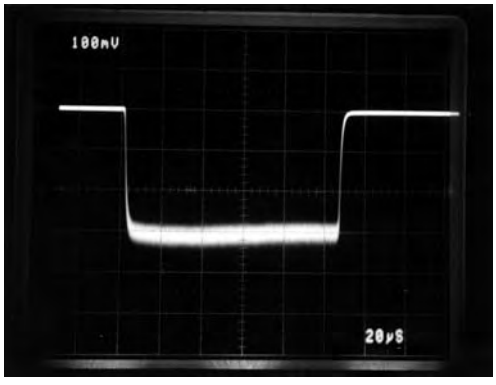

THBV3_0443EA

Figure 4-43: Change in signal-to-noise ratio for R329 when light level and load resistance are changed

The above description ignores the dark current. Taking into account the contribution of the cathode equivalent dark current (Id) and the noise current (N_A) of the amplifier circuit, Eq. 4-30 can be rewritten as follows:

$$\text{SN ratio} = \frac{I_k}{(2eB\cdot\delta/(\delta-1)\cdot(I_k+2I_d)+N^2_A)^{1/2}} \quad \cdots\cdots \text{(Eq. 4-32)}$$

In cases in which the noise of the amplifier circuit is negligible (N_A=0), the signal-to-noise ratio becomes

$$\text{SN ratio} = \frac{I_k}{(2eB\cdot\delta/(\delta-1)\cdot(I_k+2I_d))^{1/2}} \quad \cdots\cdots \text{(Eq. 4-33)}$$

where $I_k=\eta\cdot e\cdot P\cdot\lambda\ldots/hc$, and each symbol stands for the following:

I_k: cathode current (A)
λ: wavelength (m)
c: velocity of light (m/s)
P: power (W)
δ: secondary emission ratio
I_d: cathode equivalent dark current (A)
e: electron charge (C)
h: Planck's constant (J·s)
η: quantum efficiency
B: bandwidth (Hz)
N_A: noise of amplifier circuit (A)

If F=(δ/(δ-1)) is inserted in Eq. 4-33, then

$$\text{SN ratio} = \frac{I_k}{(2\cdot e\cdot(I_k+2\cdot I_d)F\cdot B)^{1/2}} = \frac{I_k\cdot\mu}{(2e(I_{ph}+2I_d)FB\cdot\mu^2)^{1/2}}$$

$$= \frac{I_p}{\sqrt{2e(I_p+2I_{da})\mu FB}} = \frac{S_pPi}{\sqrt{2e(S_pPi+2I_{da})\mu FB}}$$

where Ip is the anode signal current and Ida is the anode dark current.

Ip is given by: $Ip = Ih \cdot \mu = Sp \cdot Pi$

where Sp is the anode radiant sensitivity and Pi is the incident light power.

If the signal-to-noise ratio is 1, then

$$S_pPi = \sqrt{2e(S_pPi+2I_{da})\mu FB}$$

This relation is expressed as follows to find the variable Pi that gives

$$(S_pPi)^2 - 2e(S_pPi+2I_{da})\mu FB = 0$$

$$S_pPi = \frac{-(-2eS_p\mu FB) \pm \sqrt{(-2eS_p\mu FB)^2 - 4S_p{}^2(-4eI_{da}\mu FB)}}{2Sp^2}$$

Therefore, Pi becomes

$$Pi = \frac{e\mu FB}{Sp} + \frac{\sqrt{(e\mu FB)^2 + 4eI_{da}\mu FB}}{Sp}$$

This is the detection limit.

Detection limits at different bandwidths are plotted in Figure 4-44. When compared to ENI (obtained from Eq. 4-21) that takes into account only the dark current, the difference is especially significant at higher bandwidths. The detection limit can be approximated as ENI when the frequency bandwidth B of the circuit is low (up to about a few kilohertz), but it is dominated by the shot noise component originating from signal light at higher bandwidths.

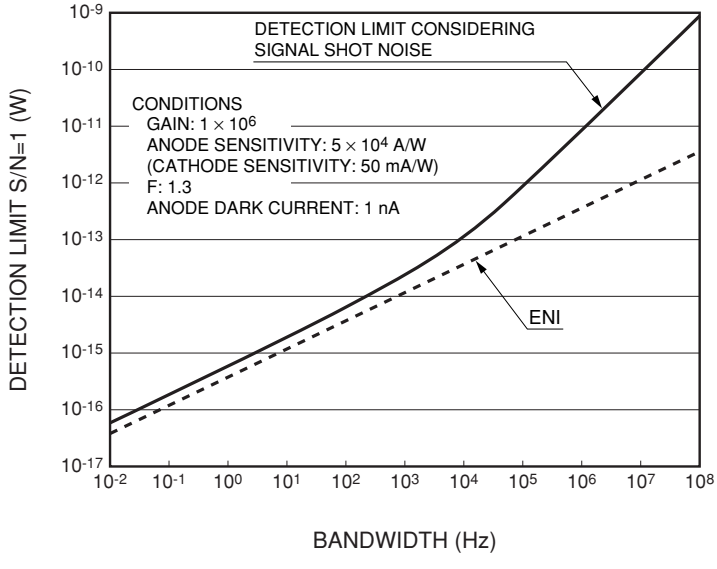

Figure 4-44: Detection limit considering signal shot noise component

Note that ENI is practical when the frequency bandwidth B of the circuit is low (up to about a few kilohertz), but is meaningless at higher bandwidths since the detection limit is dominated by the shot noise resulting from signal light. (Refer to Chapter 6, "Photon Counting".

4.3.8 Afterpulsing

When a photomultiplier tube is operated in a pulse detection mode as in scintillation counting or in laser pulse detection, spurious pulses with small amplitudes may be observed. Since these pulses appear after the signal output pulse, they are called afterpulses. Afterpulses often disturb accurate measurement of low level signals following a large amplitude pulse, degrade energy resolution in scintillation counting (See Chapter 7.), and causes errors in pulse counting applications.

Types of afterpulses

There are two types of afterpulses: one is output with a very short delay (several nanoseconds to several tens of nanoseconds) after the signal pulse and the other appears with a longer delay ranging up to several microseconds, each being generated by different mechanisms. In general, the latter pulses appearing with a long delay are commonly referred to as afterpulses.

Most afterpulses with a short delay are caused by elastic scattering electrons on the first dynode. The probability that these electrons are produced can be reduced to about one-tenth in some types of photomultiplier tubes by placing a special electrode near the first dynode. Usually, the time delay of this type of afterpulse is small and hidden by the time constant of the subsequent signal processing circuit, so that it does not create significant problems in most cases. However, this should be eliminated in time-correlated photon counting for measuring very short fluorescence lifetime, laser radar (LIDAR), and fluorescence or particle measurement using an auto correlation technique.

In contrast, afterpulses with a longer delay are caused by the positive ions which are generated by the ionization of residual gases in the photomultiplier tube. These positive ions return to the photocathode (ion feedback) and produce many photoelectrons which result in afterpulses. The amplitude of this type of afterpulse depends on the type of ions and the position where they are generated. The time delay with respect to the signal output pulse ranges from several hundred nanoseconds to over a few microseconds, and depends on the supply voltage for the photomultiplier tube. Helium gas is known to produce afterpulses because it easily penetrates through a silica bulb, so use caution with operating environments. Afterpulses can be reduced temporarily by aging (See 4.3.4, "Stability".), but this is not a permanent measure.

In actual measurements, the frequency of afterpulses and the amount of charge may sometimes be a problem. The amount of output charge tends to increase when the photomultiplier tube is operated at a higher supply voltage, to obtain a high gain, even though the number of generated ions is the same. In pulse counting applications such as photon counting, the frequency of afterpulses with an amplitude higher than a certain threshold level will be a problem.

As explained, afterpulses appear just after the signal pulse. Depending on the electrode structure, another spurious pulse (prepulse) may be observed just before the signal pulse output. But, this pulse is very close to the signal pulse and has a low amplitude, causing no problems.

4.3.9 Polarized-light dependence

Photomultiplier tube sensitivity may be affected by polarized light.[43) 44)] Tube characteristics must be taken into account when measuring polarized light. Also it should be noted that light may be polarized at such optical devices as monochromators. When polarized light enters the photocathode of a photomultiplier tube, the photocathode reflectance varies with the angle of incidence. This effect is also greatly dependent on the polarization component as shown in Figure 4-45. In this figure, Rp is the polarization component parallel to the photocathode surface (P component) and Rs is the polarization component perpendicular to the photocathode surface (S component). It is clear that the photocathode reflectance varies with the angle of incidence. Because this figure shows the calculated examples with the assumption that the absorption coefficient at the photocathode is zero, the actual data will be slightly more complicated.

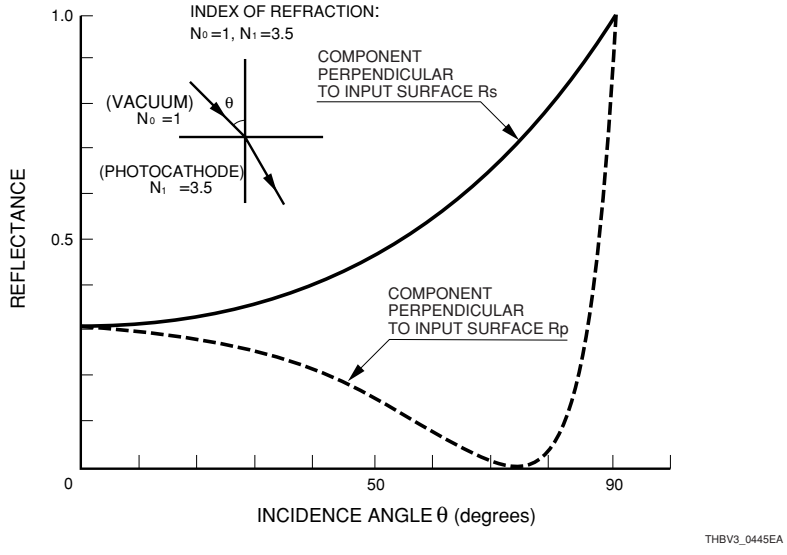

Figure 4-45: Angle dependence of reflectance

If the polarization plane of the incident light has an angle θ with respect to the perpendicular of the photocathode surface, the photocurrent I θ is given by the following expression:

$$I\theta = I_S \cos^2\theta + I_P \sin^2\theta = \frac{I}{2}(I_P+I_S)\left(1-\frac{I_P-I_S}{I_P+I_S}\cdot\cos^2\theta\right) \quad \text{(Eq. 4-34)}$$

where

I_S: Photocurrent produced by polarized component perpendicular to the photocathode
I_P: Photocurrent produced by polarized component parallel to the photocathode

while

$$I_O = \frac{I_P+I_S}{2},\ P = \frac{I_P-I_S}{I_P+I_S} \quad \text{(Eq. 4-35)}$$

then substituting Eq. 4-35 into Eq. 4-34 gives the following relationship

$$\theta = I_O(1-P\cdot\cos^2\theta) \quad \text{(Eq. 4-36)}$$

P is called the polarization factor and indicates the polarized-light dependence of a photomultiplier tube, and is measured using the optical system like that shown in Figure 4-46.

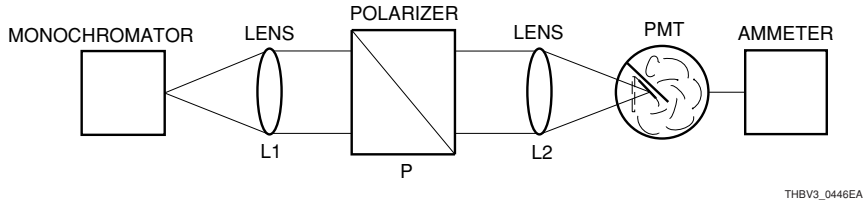

Figure 4-46: Optical system used for measuring polarized-light dependence

In the above measurement, monochromatic light from the monochromator is collimated by L_1 (collimator lens) and is linearly polarized by the polarizer (P). The polarized light is then focused onto the photomultiplier tube through L_2 (condenser lens). The dependence on the polarized light is measured by recording the photomultiplier tube output in accordance with the rotating angle of the polarizer.

In this case, the polarization component of the light source must be removed. This is done by interposing a diffuser plate such as frosted glass or by compensating for the photomultiplier tube output values measured when the tube is at 0 degree and is then rotated to 90 degrees with respect to the light axis.

Figure 4-47 illustrates the polarized-light dependence of a side-on photomultiplier tube with a reflection type photocathode. In principle, this dependence exists when the light enters slantways with respect to the photocathode surface. In actual operation, the polarization factor P is almost zero when the light enters perpendicular to the transmission type photocathode surface.

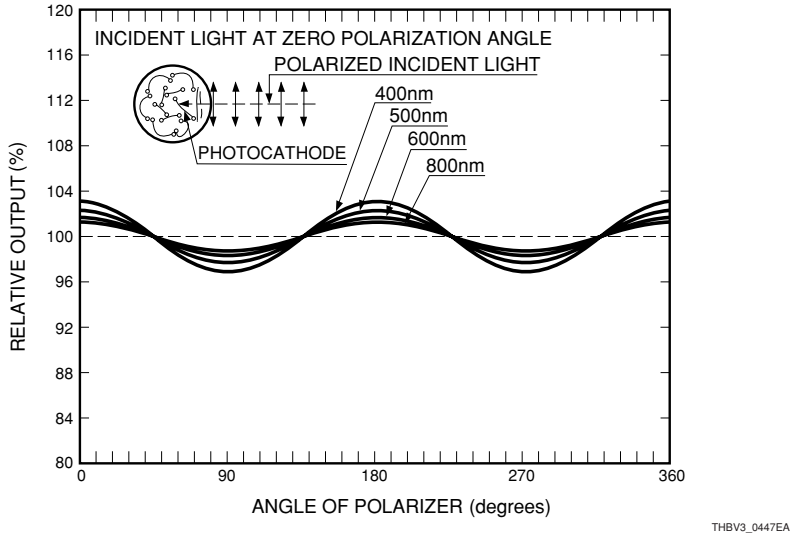

Figure 4-47: Typical polarization-light dependence of a side-on photomultiplier tube

In the case of reflection-type photocathode photomultiplier tubes, because the photocathode is arranged at a certain angle with respect to the input window, the sensitivity is affected by polarized light. Figure 4-48 indicates the relative output of a reflection-type photocathode photomultiplier tube as a function of the angle of incident light. It can be seen that the polarization factor P becomes smaller as the direction of the incident light nears the perpendicular of the photocathode surface.

The reflection-type photocathode photomultiplier tubes usually exhibit a polarization factor of about 10 percent or less, but tubes specially designed to minimize the polarization-light dependence offer three percent or less. A single crystal photocathode such as gallium arsenide (GaAs) has high reflectance and show a polarization factor of around 20 percent, which is higher than that of alkali antimonide photocathodes.

The polarization that provides the maximum sensitivity is the component perpendicular to the tube axis (P component). In contrast, the polarization that gives the minimum sensitivity is the component parallel to the tube axis (S component), independent of the type of tube and wavelength of incident light. As can be seen from Figure 4-45, this is probably due to a change in the photocathode transmittance. The S component increases in reflectance as the angle of incidence becomes larger, whereas the P component decreases. Moreover, as the wavelength shifts to the longer side, the reflectance generally decreases and the polarization factor P becomes smaller accordingly, as shown in Figure 4-47.

In applications where the polarized-light dependence of a photomultiplier tube cannot be ignored, it will prove effective to place a diffuser such as frosted glass or tracing paper in front of the input window of the photomultiplier tube or to use a photomultiplier tube with a frosted window.

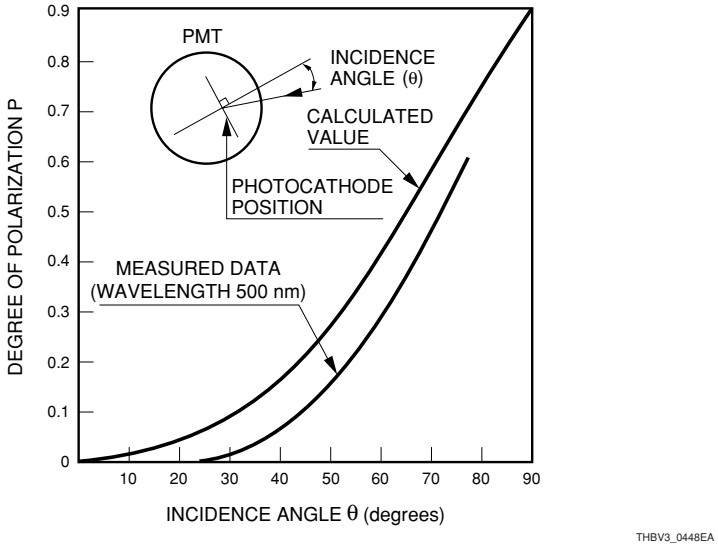

Figure 4-48: Relative output vs. incident angle of polarized light

References in Chapter 4

1) Hamamatsu Photonics Catalog: Photomultiplier Tubes.
2) T. Hiruma, SAMPE Journal. 24, 35 (1988).
3) A. H. Sommer: Photoemissive Materials, Robert E. Krieger Publishing Company (1980).
4) T. Hirohata and Y. Mizushima: Japanese Journal of Applied Physics. 29, 8, 1527 (1990).
5) T. Hirohata, T. Ihara, M. Miyazaki, T. Suzuki and Y. Mizushima: Japanese Journal of Applied Physics. 28, 11, 2272 (1989).
6) W.A. Parkhurst, S. Dallek and B.F. Larrick: J. Electrochem. Soc, 131, 1739 (1984).
7) S. Dallek, W.A. Parkhurst and B.F. Larrick: J. Electrochem. Soc, 133, 2451 (1986).
8) R.J. Cook: Phys. Rev. A25, 2164; 26,2754 (1982).
9) H.J. Kimble and L. Mandel: Phys. Rev. A30, 844 (1984).
10) M. Miyao, T. Wada, T. Nitta and M. Hagino: Appl. Surf. Sci. 33/34, 364 (1988).
11) Tailing Guo: J. Vac. Sci. Technol. A7, 1563 (1989).
12) Huairong Gao: J. Vac. Sci. Technol. A5, 1295 (1987).
13) C.A. Sanford and N.C. MacDonald: J. Vac. Sci. Technol. B 6. 2005 (1988).
14) C.A. Sanford and N.C. MacDonald: J. Vac. Sci. Technol. B 7. 1903 (1989).
15) M. Domke, T. Mandle, C. Laubschat, M. Prietsch and G.Kaindl: Surf. Sci. 189/190, 268 (1987).
16)M. Niigaki, T. Hirohata, T. Suzuki, H. Kan and T. Hiruma: Appl. Phys. Lett. 71 (17) 27, Oct. 1997
17) K. Nakamura, H. Kyushima: Japanese Journal of Applied Physics, 67, 5, (1998)
18) D. Rodway: Surf. Sci. 147, 103 (1984).
19) "Handbook of Optics": McGraw-Hill (1978).
20) James A. R. Samson: "Techniques of Vacuum Ultraviolet Spectroscopy" John Wiley & Sons, Inc (1967).
21) C.R. Bamford: Phys. Chem. Glasses, 3, 189 (1962).
22) Corning Glass Works Catalog.
23) IEEE ET-61A 1969.5.8.
24) IEEE STD 398-1972.
25) IEC PUBLICATION 306-4, 1971.
26) H. Kume, K. Koyama, K. Nakatsugawa, S. Suzuki and D. Fatlowitz: Appl. Opt, 27, 1170 (1988).
27) T. Hayashi:"PHOTOMULTIPLIER TUBES FOR USE IN HIGH ENERGY PHYSICS". Hamamatsu Photonics Technical Publication (APPLICATION RES-0791-02).
28) Hamamatsu Photonics Technical Publication "USE OF PHOTOMULTIPLIER TUBES IN SCINTILLATION APPLICATIONS" (RES-0790)
29) T.H. Chiba and L. Mmandel: J. Opt. Soc. Am. B,5, 1305 (1988).
30) D.P. Jones: Appl. Opt. 15,14 (1976).
31) D.E. Persyk: IEEE Trans. Nucl. Sci. 38, 128 (1991).
32) Mikio Yamashita: Rev. Sci. Instum., 49, 9 (1978).
33) "Time-Correlated Single-Photon Counting": Acadenic Press, Inc (1985).
34) G.F.Knoll: "RADIATION DETECTION and MEASUREMENT", John Wiley & Sons, Inc. (1979).
35) C.E. Miller, et al.: IEEE Trans. Nucl. Sci. NS-3, 91 (1956).
36) A.T. Young: Appl. Opt., 8, 12, (1969).
37) R.L. Bell: "Negative Electron Affinity Devices", Clarendon Press. Oxford (1973).
38) G.A. Morton et al.: IEEE Trans. Nucl. Sci. NS-14 No.1, 443 (1967).
39) R. Staubert et al.: Nucl. Instrum. & Methods 84, 297 (1970).
40) S.J. Hall et al.: Nucl. Instrum. & Methods 112, 545 (1973).
41) Illes P. Csorba "Image Tubes" Howard W, Sams & Co (1985).
42) F. Robber: Appl. Opt., 10, 4 (1971).
43) S.A. Hoenig and A. Cutler ÅE: Appl. Opt. 5,6, 1091 (1966).
44) H. Hora: Phys. Stat. Soli Vol (a), 159 (1971).

MEMO